# Palmitate is increased in the cerebrospinal fluid of obese humans and induces memory impairment in mice via pro-inflammatory TNF-$\alpha$

Helen M Melo, Gisele da S Seixas da Silva, Marcella Ramos Sant'Ana, Camila Vieira, Ligo Teixeira, Julia R Clarke, Vivian S Miya Coreixas, Bruno C de Melo, Juliana T S Fortuna, Leticia Forny-Germano, et al.

# Palmitate is increased in the cerebrospinal fluid of obese humans and induces memory impairment in mice via pro-inflammatory TNF-α

Helen M. Melo[1], Gisele da S. Seixas da Silva[2], Marcella Ramos Sant'Ana [3], Camila Vieira Ligo Teixeira[4], Julia R. Clarke[5], Vivian S. Miya Coreixas[1], Bruno C. de Melo[1], Juliana T. S. Fortuna[1], Leticia Forny-Germano[1], José Henrique Ledo[1], Maíra S. Oliveira[1], Claudia P. Figueiredo[5], Raphaelle Pardossi-Piquard[6], Frédéric Checler[6], José María Delgado-García[7], Agnès Gruart[7], Licio A. Velloso[8], Marcio L. F. Balthazar [4], Dennys E. Cintra[3], Sergio T. Ferreira[1,9] and Fernanda G. De Felice[1,10,11*]

[1] Institute of Medical Biochemistry Leopoldo de Meis, Federal University of Rio de Janeiro, Rio de Janeiro, RJ 21941-902, Brazil.

[2] Federal Institute of Education, Science and Technology of Rio de Janeiro, Rio de Janeiro, RJ 20270-021, Brazil.

[3] Laboratory of Nutritional Genomics (LabGeN), School of Applied Sciences); CELN - Nutrigenomics and Lipids Research Center, School of Applied Sciences, University of Campinas (UNICAMP), Limeira, SP 13484-350, Brazil

[4] Brazilian Institute of Neuroscience and Neurotechnology, BRAINN; Department of Neurology, Neuroimaging Laboratory, University of Campinas (UNICAMP), Campinas, SP 13083-887, Brazil.

[5] School of Pharmacy, Federal University of Rio de Janeiro, Rio de Janeiro, RJ 21941-902, Brazil.

[6] Université Côte d'Azur, INSERM, CNRS/UMR7275, IPMC, team labeled "Laboratory of Excellence (LABEX) Distalz", 660 route des Lucioles, 06560, Sophia-Antipolis, Valbonne, France.

[7] Division of Neuroscience, Pablo de Olavide University, Seville-41013, Spain.

[8] Laboratory of Cell Signalling, Obesity and Comorbidities Research Centre, University of Campinas, Campinas, SP 13084-761, Brazil.

[9] Institute of Biophysics Carlos Chagas Filho, Federal University of Rio de Janeiro, Rio de Janeiro, RJ 21941-902, Brazil.

[10] Centre for Neuroscience Studies & Department of Psychiatry, Queen's University, Kingston, ON K7L 3N6, Canada.

[11] Lead Contact

* Correspondence: felice@bioqmed.ufrj.br

**Summary**

Obesity has been associated with cognitive decline, atrophy of brain regions related to learning and memory, and higher risk of developing dementia. However, the molecular mechanisms underlying these neurological alterations are still largely unknown. Here, we investigate the effects of palmitate, a saturated fatty acid present at high amounts in fat-rich diets, in the brain. Palmitate was increased in the cerebrospinal fluid (CSF) of overweight and obese patients with amnestic mild cognitive impairment. In mice, intracerebroventricular infusion of palmitate impaired synaptic plasticity and memory. Palmitate induced astroglial and microglial activation in the hippocampus of mice, and its deleterious impact was mediated by microglia-derived TNF-α signaling. Results establish that obesity is associated with increases in CSF palmitate. By defining a pro-inflammatory mechanism by which abnormal levels of palmitate in the brain impair memory, results further suggest that anti-inflammatory strategies may constitute an approach to attenuate memory impairment in obesity.

## Introduction

Worldwide obesity has nearly tripled in the past four decades. In 2016, more than 1.9 billion adults were overweight and over 650 million were obese (WHO, 2018). Overweight and obesity states are defined by abnormal or excessive fat accumulation that may impair health (WHO, 2018), and are frequently associated with metabolic and cardiovascular disorders. Diabetes, dyslipidemia and hypertension often overlap in overweight and obese humans (Chan et al., 1994; Guh et al., 2009; Hu et al., 2001; Janssen et al., 2002; Mokdad et al., 2003; Must et al., 1999; Wilson et al., 2002). Obesity and/or increased fat intake are linked to cognitive decline and a higher risk of developing dementia (Kalmijn et al., 2004; Kivipelto et al., 2005).

Individuals become overweight and/or obese when there is an imbalance between calories consumed and calories expended, often when an increased intake of unbalanced diets high in fat is combined with decreased physical activity (Spiegelman and Flier, 2001). In obesity-related insulin resistance and type 2 diabetes (T2D), consumption of high-fat meals results in excess serum levels of saturated fatty acids (SFAs) (Meek et al., 1999; Roust and Jensen, 1993) which impair metabolism and cause peripheral insulin resistance (Fernández-Real et al., 2003; Mayer et al., 1993; Parker et al., 1993; Vessby et al., 2001). Palmitate is the most abundant SFA present in the circulation (Quehenberger et al., 2010), and also in the cerebrospinal fluid (CSF) (Pilitsis et al., 2001). Increased brain uptake and accumulation of palmitate was reported in obese patients with metabolic syndrome (Karmi et al., 2010). In mice, SFAs, including palmitate, have been shown to affect the hypothalamus, a key regulator of peripheral metabolic homeostasis (Milanski et al., 2009; Thaler et al., 2012; Valdearcos et al., 2014). Palmitate has been related to insulin resistance, endoplasmic

reticulum stress and increased pro-inflammatory response in the hypothalamus of mice (Benoit et al., 2009; Cheng et al., 2015; Marwarha et al., 2016). However, it remains unclear whether palmitate is increased in the central nervous system of overweight or obese humans, and if it interferes with mechanisms of synaptic plasticity and memory.

We hypothesized that palmitate levels in the central nervous system could be altered in obesity and that palmitate could affect brain regions involved in learning and memory. We found that palmitate levels were increased in the CSF of overweight and obese humans with amnestic mild cognitive impairment (aMCI). Elevated CSF palmitate levels were associated with decreased cognitive performance in overweight individuals with diabetes, dyslipidemia and/or hypertension. When infused into the lateral brain ventricle of mice, palmitate impaired synaptic plasticity and memory. Palmitate reduced insulin expression and induced phosphorylation of neuronal insulin receptor substrate 1 (IRS-1) at multiple inhibitory serine residues in primary hippocampal cultures. Palmitate further activated astrocytes and microglia *in vitro* and in the hippocampi of mice, and caused an increase in hippocampal TNF-α levels. Minocycline, a tetracycline antibiotic commonly used to inhibit microglial activation, protected against palmitate-induced cognitive impairment. Palmitate failed to cause cognitive impairment in mice treated with infliximab, a monoclonal TNF-α-neutralizing antibody, and in TNF-α receptor knock-out ($TNFR1^{-/-}$) mice, indicating that TNF-α signaling underlies the deleterious impact of palmitate on memory. Results establish a mechanism leading to memory deficits triggered by palmitate and provide a rational basis for the increased risk of cognitive decline in obese individuals.

## Results

### Palmitate is increased in the cerebrospinal fluid (CSF) of overweight and obese humans

Because it has not been demonstrated whether levels of palmitate in the CNS are altered in overweight or obese humans, we initially measured palmitate levels in the CSF from normal weight, overweight and obese individuals with aMCI (Teixeira et al., 2016, 2018). We found that palmitate levels were increased in the CSF of overweight and obese humans (Figure 1A; normal weight, N = 14; overweight, N = 26; obese, N = 9; ****$p < 0.0001$, one-way ANOVA followed by Holm-Sidak's *post hoc* test). CSF palmitate levels further showed positive correlations with body mass index (BMI) and with abdominal circumference in individuals with aMCI (Figure 1B, C; N = 49 subjects; **** $p < 0.0001$, linear regression). This correlation was observed in men and women (Figure S1A-D; N = 16 males/33 females; *$p < 0.05$ (male); ****$p < 0.0001$ (female), linear regression). We next stratified this cohort into patients affected or not by diabetes, dyslipidemia and/or hypertension, conditions that usually overlap in overweight and obese patients. Only 2 out of 14 normal weight subjects had diabetes, dyslipidemia or hypertension. On the other hand, 6 out of 9 obese subjects had diabetes, dyslipidemia and/or hypertension. Among overweight humans we found a more equilibrate proportion of individuals with (N = 15) and without (N = 11) diabetes, dyslipidemia and/or hypertension (Table S1). We found that overweight individuals with diabetes, dyslipidemia or hypertension exhibited a trend of increase in CSF palmitate compared to overweight individuals not affected by these co-morbid conditions (Figure 1D; individuals with diabetes, dyslipidemia and/or hypertension, N = 15; individuals without diabetes, dyslipidemia and/or hypertension, N = 11; $p = 0.095$, unpaired t-test).

CSF palmitate correlated inversely with cognitive performance in overweight individuals. We initially found a trend of decrease in mini-mental state examination (MMSE) scores for overweight subjects with diabetes, dyslipidemia and/or hypertension compared to individuals without these conditions (Figure S1E; patients with diabetes, dyslipidemia and/or hypertension, N = 15; patients without diabetes, dyslipidemia and/or hypertension, N = 11; $p = 0.099$, unpaired t-test). We next observed that CSF palmitate correlated inversely and significantly with MMSE score in overweight subjects affected by diabetes, dyslipidemia and/or hypertension (Figure 1E; N = 14; $*p < 0.05$, linear regression), but not in overweight subjects without these conditions (Figure 1F; N = 11, no statistical significance, linear regression). Overall, these results indicate that obesity is associated with increased CSF palmitate levels in humans. Results further show that CSF palmitate is elevated in overweight individuals with diabetes, dyslipidemia and/or hypertension and is associated with decreased cognitive performance.

**Palmitate inhibits synaptic plasticity and impairs memory in mice**

Numerous studies in humans and animal models indicate that obesity and a diet rich in saturated fatty acids are linked to deficits in learning and memory (Arnold et al., 2014; Knight et al., 2014; Whitmer et al., 2008) and we next sought to investigate possible mechanisms associated with these effects. We first evaluated the impact of palmitate on synaptic plasticity by analyzing the induction and maintenance of hippocampal (CA3-CA1 synapses) long-term potentiation (LTP) in alert behaving adult mice. Compared to control (vehicle-infused) mice, field excitatory post-synaptic potentials (fEPSPs) were reduced in

mice that received a stereotaxic infusion of palmitate (0.3 nmol) into the dorsal hippocampus 10 days prior to recordings (Figure 2A, B; N = 6 vehicle-infused/N= 8 palmitate-infused mice; ****$p < 0.0001$, unpaired t-test). Moreover, recordings on subsequent days revealed that palmitate persistently impaired the LTP response (Figure 2C; N = 6 vehicle-infused/N= 8 palmitate-infused mice; * $p < 0.05$, two-way ANOVA followed by Holm-Sidak's *post hoc* test). In control experiments, mice that received an intracerebroventricular (i.c.v.) infusion of the monounsaturated fatty acid, oleic acid, presented normal LTP response and maintenance 10 days after infusion (Figure S2A-B, N = 6 vehicle-infused/N= 4 oleate-infused mice; no statistical significance).

We next examined the effects of an i.c.v. infusion of palmitate on memory. Ten days after i.c.v. infusion of palmitate, mice presented memory deficits in novel object recognition (NOR), novel object location (NOL) and step-down inhibitory avoidance (IA) tests (Figure 2D-F; NOR: vehicle (N = 7), palmitate (N = 7), ***$p < 0.0005$, unpaired t-test comparing exploration times in the novel object; NOL: vehicle (N = 9), palmitate (N = 8), ****$p < 0.0001$, unpaired t-test comparing exploration times in the NOL; IA: vehicle (N = 11), palmitate (N = 9), **$p < 0.005$, Mann-Whitney test).

Palmitate-infused mice also showed memory impairment in the NOR test 24 hours after infusion (Figure S2C; vehicle (N =10), palmitate (N = 9), ***$p < 0.001$, unpaired t-test comparing exploration times in the novel object). In contrast, mice that received an i.c.v. infusion of oleic acid presented normal performances in the NOR test both 24 hours and 10 days after infusion (Figure S2D, E; NOR 24h: vehicle (N =10), oleate (N = 10); NOR 10 days: vehicle (N = 10), oleate (N = 10); no statistically significant differences comparing exploration times in the novel object).

Palmitate further impaired memory in the Barnes maze task, as revealed by an increased primary latency and a trend, albeit not statistically significant, increase in errors by palmitate-infused mice at the fourth (last) day of training and reduced time spent in the target zone during the test phase (Figure 2 G-I; latency (training): vehicle (N = 7), palmitate (N = 6), **p < 0.005, two-way ANOVA followed by Sidak's *post hoc* test; errors (training): vehicle (N = 7), palmitate (N = 6), p = 0.09, two-way ANOVA followed by Sidak's *post hoc* test; time in target zone (test): vehicle (N = 7), palmitate (N = 6), **p < 0.005, unpaired t-test).

No statistically significant differences were observed in average weights between vehicle- and palmitate-infused mice (Figure S2F, N = 6 vehicle-infused/N= 5 palmitate-infused mice). In addition, control measurements of total distance travelled (Figure S2G) and average speed (Figure S2H) during the Barnes maze task training phase, as well as the number of crossings in an open field arena ten days after i.c.v. infusion (Figure S2I), showed that palmitate did not affect locomotor activity of mice. Furthermore, ten days after infusion, no differences in the total amount of time spent exploring the two objects in the NOR test were detected between vehicle- and palmitate-infused mice, indicating no impact on motivation or exploratory behavior (Figure S2J). Altogether, assessment of memory employing various tests indicated that i.c.v. palmitate induced memory impairment in mice.

We next investigated whether palmitate altered synaptic proteins in mice. Immunoreactivity of the pre-synaptic marker protein, synaptophysin, was reduced in the hippocampus of mice ten days after i.c.v. infusion of palmitate (Figure S3A; vehicle (N = 9), palmitate (N =9), *p < 0.05, unpaired t-test). No differences were observed for the post-

synaptic marker protein, PSD-95 10 days after palmitate infusion (Figure S3B; vehicle (N = 5, palmitate (N = 5), no statistically significant difference).

**Palmitate inhibits neuronal IRS-1 signaling via microglial activation *in vitro***

Both *in vitro* and *in vivo* studies have indicated that insulin regulates neuronal survival, acts as a growth factor, and regulates circuit function and plasticity (Chiu et al., 2008; Lee et al., 2011; Zhao et al., 2010). These findings prompted us to analyze whether palmitate would impact neuronal insulin signaling in primary hippocampal cultures (containing ~ 50 % neurons, 50 % non-neuronal cells, largely astrocytes and microglia). Exposure to palmitate (200 μM for 24 hours) triggered a marked reduction in insulin expression (Figure 3A; N = 3 independent cultures; **$p < 0.005$, paired t-test) in the absence of changes in cell viability for up to 48 hours (Figure S4A, B; N = 5 independent cultures; *$p < 0.05$, one-way ANOVA followed by Dunnett's *post-hoc* test). Previous studies have used similar concentrations of palmitate to induce insulin resistance in hypothalamic cells (Mayer and Belsham, 2010) and increased cytokine levels in purified astrocyte culture (Liu et al., 2013).

Hippocampal neurons exposed to palmitate further showed decreased IRS-1 phosphorylation at tyrosine residue 612 (Figure 3B-C; N = 4 independent cultures; *$p < 0.05$, unpaired t-test) and increased phosphorylation at inhibitory serine residues 636 (IRS-1pSer636), 307 (IRS-1pS307) and 312 (IRS-1pS312) (Figure 3D-I; IRS-1pSer636, N = 4 independent cultures; IRS-1pSer307, N = 3 independent cultures; IRS-1pSer312, N = 3 independent cultures; *$p < 0.05$, unpaired t-test). Interestingly, no differences were observed

in IRS-1pSer636 in hippocampal neurons exposed to oleate (Figure S4 C-D; N = 3 independent cultures).

**Palmitate induces hippocampal inflammation**

Landmark studies have shown that inflammation is a key mechanism underlying impaired peripheral insulin signaling in obesity and T2D (Hotamisligil and Spiegelman, 1994; Hotamisligil et al., 1993, 1996). Specifically, hypothalamic inflammation has been associated with obesity (Milanski et al., 2009; Thaler et al., 2012). Thus, we next investigated if palmitate could cause hippocampal inflammation. We found that exposure of hippocampal cultures to palmitate (200 μM for 4 hours) induced an increase in GFAP immunoreactivity (Figure 4A-B; N = 3 independent cultures; **p = 0.008, unpaired t-test). Similarly, palmitate caused hippocampal astrogliosis in mice 10 days after i.c.v infusion (Figure 4 C-D; N= 6 per group, *p < 0.05, unpaired t-test).

Using purified microglial cultures, we found that exposure to palmitate (200 μM for 2 hours) induced microglial activation, as indicated by increased Iba-1 immunoreactivity and average cell area (Figure 4 E-G; N = 3 independent cultures, **p < 0.005, *p < 0.05, unpaired t-test). Similarly, palmitate increased the number of Iba-1 positive cells in the hippocampi of palmitate-infused mice (Figure 4 H-I; N = 5 vehicle-infused, N = 6 palmitate-infused mice; ** p = 0.0057, unpaired t-test). Control experiments showed that exposure to oleate had no effect on Iba-1 immunoreactivity or average cell area in microglial cultures and that microglial activation obtained by palmitate treatment was similar to that induced by LPS

(Figure S5A-C; N = 3 independent cultures, *p < 0.05, one-way ANOVA followed by Holm-Sidak's post hoc test).

**Microglia is implicated in palmitate-induced memory impairment**

Microglial activation induced by palmitate was fully blocked by the tetracycline antibiotic, minocycline (Figure 5 A-C; N = 3 independent cultures, *p < 0.05, two-way ANOVA followed by Holm-Sidak's *post hoc* test). To determine whether palmitate-induced activation of a microglial inflammatory response could lead to increased IRS-1 phosphorylation in neurons, we exposed hippocampal cultures to conditioned medium from purified microglial cultures that had been previously exposed to palmitate (200 μM for 2 hours). Microglial conditioned medium (MCM) induced an increase in neuronal IRS-1pSer636 (Figure 5D, E; N = 3 independent cultures; *p < 0.05, unpaired t-test), and this increase was fully prevented by minocycline in hippocampal neurons exposed to palmitate (Figure 5F, G; N = 3 independent cultures, *p < 0.05; **p < 0.005; two-way ANOVA followed by Holm-Sidak's *post hoc* test).

Palmitate failed to cause memory impairment in mice treated with minocycline (50 mg/kg/d, IP, for 3 consecutive days ending on the day of vehicle or palmitate i.c.v. infusion) (Figure 5H; vehicle (N = 10), palmitate (N = 7), vehicle plus minocycline (N = 9), palmitate plus minocycline (N = 8), *p < 0.05; **p =0.005; ***p < 0.001 (Two-way ANOVA followed by Holm-Sidak's *post hoc* test comparing exploration times in the novel object). Moreover, while palmitate increased the number of Iba-1 positive cells in the hippocampi of control mice, no increase was observed when mice that received palmitate were treated with

minocycline (Figure 5I-J; vehicle (N = 9), palmitate (N = 11), vehicle plus minocycline (N = 4), palmitate plus minocycline (N = 4), ** $p < 0.005$, two-way ANOVA followed by Dunnett's *post hoc* test).

**Pro-inflammatory TNF-α mediates palmitate-induced cognitive impairment in mice**

Palmitate has been shown to increase the expression of TNF-α in adipocyte and muscle cells (Ajuwon and Spurlock, 2005; Jové et al., 2006). We found that exposure of hippocampal cultures to palmitate (200 μM for 4 hours) induced an increase in TNF-α in the medium (Figure 6A; N = 8 independent cultures, significance of pairing: correlation coefficient (r) = 0.94, ***$p < 0.0001$; **$p = 0.006$, paired t-test).

We further found that palmitate induced an increase in TNF-α mRNA and protein levels in the hippocampus that could be detected 24 hours after infusion in mice (Figure 6B, C; mRNA: vehicle (N = 11), palmitate (N = 8); protein: vehicle (N = 10), palmitate (N = 14); *$p < 0.05$, unpaired t-test). TNF-α mRNA (but not protein levels) remained elevated 10 days after infusion of palmitate (Fig. 6D, E; mRNA: vehicle (N = 6), palmitate (N = 4); *$p < 0.05$ (unpaired t-test); protein: vehicle (N = 9), palmitate (N = 10), no statistically significant difference, unpaired t-test).

Neuronal IRS-1pSer636 induced by palmitate in hippocampal cultures was prevented by infliximab (1 μg/ml), a TNF-α neutralizing monoclonal antibody, suggesting that increased TNF-α secreted by microglia mediates the inhibition of neuronal IRS-1 signaling

induced by palmitate (Figure 6 F-G; N = 3 independent cultures, **p < 0.005; two-way ANOVA followed by Holm-Sidak's *post hoc* test).

We next asked whether a strategy to attenuate abnormally increased TNF-α signaling could alleviate memory impairment induced by palmitate. To test this hypothesis, we carried out an i.c.v. injection of the infliximab (10 ng in 1 μl) 1 hour before the infusion of palmitate in mice. Infliximab completely prevented palmitate-induced NOR memory deficits both 24 hours and 10 days post-infusion, suggesting that TNF-α mediates palmitate-induced cognitive impairment (Figure 6H-I; 24 h: vehicle (N = 10), palmitate (N = 10), vehicle plus infliximab (N = 9), palmitate plus infliximab (N = 10), *p < 0.05, **p < 0.005, two-way ANOVA followed by Holm-Sidak's *post hoc* test comparing exploration times in the novel object); 10 days: vehicle (N = 9), palmitate (N = 9), vehicle plus infliximab (N = 10), palmitate plus infliximab (N = 10), **p < 0.005, two-way ANOVA followed by Holm-Sidak's *post hoc* test comparing exploration times in the novel object). Palmitate also did not cause microgliosis in mice treated with infliximab (Figure 6 J-K; vehicle (N = 10), palmitate (N = 12), vehicle plus infliximab (N = 5), palmitate plus infliximab (N = 6), **p < 0.005, two-way ANOVA followed by Dunnett's *post hoc* test).

We further examined whether infliximab could reverse memory impairment in mice fed a high fat diet (HFD; 35% fat content by weight). Mice fed an HFD for 12 weeks exhibited memory impairment in the NOR test (Figure 7A; normal diet (N = 9), HFD (N = 10), *p < 0.05, unpaired t-test comparing exploration times in the novel object). HFD-fed mice were then divided into two groups. One group continued to receive HFD for 4 additional weeks, while the other group received HFD for 4 additional weeks and were treated i.c.v. with infliximab (10 μg in 1 μl) for 3 consecutive days ending on the day of the NOR test.

While mice that were kept on a HFD up to 16 weeks continued to exhibit memory impairment in the NOR test, short-term treatment with infliximab reversed memory impairment induced by HFD (Figure 7 B; HFD (N = 4), HFD plus infliximab (N = 5), *p < 0.05, unpaired t-test comparing exploration times in the novel object).

**TNFR1 deletion prevents memory impairment in mice**

To further investigate the role of TNF-α in memory impairment induced by palmitate, we infused palmitate (9 nmol, i.c.v.) in $TNFR1^{-/-}$ or wild type C57BL/6 mice. Significantly, mice lacking TNFR1 were protected from memory impairment induced by palmitate both 24 hours (Figure 7C) and 8 days (Figure 7D) after infusion (24h: vehicle-infused wild type (N = 9), palmitate-infused wild type (N = 9), vehicle-infused $TNFR1^{-/-}$ (N = 9), palmitate-infused $TNFR1^{-/-}$ (N = 10); 8 days: vehicle-infused wild type (N = 10), palmitate-infused wild type (N = 10), vehicle-infused $TNFR1^{-/-}$ (N = 7), palmitate-infused $TNFR1^{-/-}$ (N = 8); *p < 0.05, **p < 0.005, ***p < 0.0005, ****p < 0.0001, two-way ANOVA followed by Holm-Sidak's *post hoc* test).

**Discussion**

Obese and T2DM patients show structural brain alterations with reduced cerebral volume, including hippocampal and cortical atrophies (Gustafson, 2006; Gustafson et al., 2004; Ho et al., 2010). Moreover, T2D and obese patients, as well as animal models of diabetes, present cognitive impairment (Elias et al., 2003; Jeon et al., 2012; Roberts et al.,

2014; Takeda et al., 2010), and T2D favors the development of dementia later in life (Ott et al., 1996).

Consumption of HFDs containing elevated amounts of SFAs induces obesity and T2D, and the association between obesity and dementia is increasingly rising concerns regarding the possible deleterious impact of unhealthy diets in the brain (Kalmijn et al., 2004; Morris et al., 2003). In animal models of obesity and AD, administration of a HFD induces cognitive impairment and accelerates AD pathology (Jeon et al., 2012; Takeda et al., 2010). Moreover, damage to blood-brain barrier permeability as well as increased palmitate levels in the brain have been observed in mice fed a HFD (Spinelli et al., 2017; Takechi et al., 2017).

Our results established that increased body weight is associated with increased CSF palmitate in humans. Results further showed that CSF palmitate is elevated in overweight individuals with diabetes, dyslipidemia and/or hypertension and, importantly, is associated with decreased cognitive performance. These findings suggest that the brain may sense alterations that occur in obesity.

In peripheral tissues, inflammatory and metabolic stress signaling cascades trigger disruption of insulin signaling (Hotamisligil et al., 1993, 1996) and palmitate induces insulin resistance in hypothalamus (Mayer and Belsham, 2010), liver (Nakamura et al., 2009) and muscle (Yuzefovych et al., 2010) cells. Our findings in hippocampal cultures indicated that palmitate disrupted insulin expression and signaling, with decreased insulin mRNA levels and IRS-1pTyr612, and increased IRS-1pSer636, pSer307 and pSer312. In line with current findings, mice fed a HFD exhibited increased immunoreactivity for IRS-1pSer616 in the hippocampus and impaired spatial memory (Arnold *et al.*, 2014). Increased palmitate levels may thus be linked to brain inflammation and impaired insulin signaling in overweight

humans with diabetes, dyslipidemia and/or hypertension, contributing to decreased cognitive performance.

Our analysis indicated that palmitate levels in the CSF ranged from 0.8–2.7 μg/ml in normal weight humans to 1.5–4.1 μg/ml and 3.8–5.9 μg/ml in overweight and obese individuals, respectively. An early study reported that healthy humans present ~ 0.64 μg palmitate/ml CSF, similar to the range we have found (Pilitsis et al., 2001). More recently, lipid profiles were evaluated in brain and plasma of post-mortem T2D elderly subjects and reported ~ 20% increase in palmitate cholesteryl esters in brain homogenates from T2D in comparison to controls (Ginneken et al., 2017). However, this study did not include a quantitative analysis of palmitate levels. Additional studies aiming at investigating levels of palmitate in the CSF and/or brains in the context of obesity are anticipated in the field.

Palmitate did not induce cognitive impairment in mice that had been treated with either infliximab or minocycline, strategies to neutralize TNF-α or microglia, respectively. These results suggest that palmitate acts on microglial cells, which likely secret soluble factors, including TNF-α, that impair memory. Peripheral inflammation in obesity and T2D involves many components of the classical inflammatory response, including abnormal production of TNFα, IL-1β and IL-6, and activation of a network of inflammatory signaling pathways (Gregor and Hotamisligil, 2011; Hotamisligil, 2017). Microglia are centrally involved in the immune response in the CNS. When activated, microglia release proinflammatory cytokines and become an antigen presenting cell (Hanisch and Kettenmann, 2007). TNF-α is increased in the serum of obese patients (Hotamisligil et al., 1995), mediates insulin resistance in obesity and T2D (Hotamisligil, 1999), and has been recently implicated in brain dysfunction in trauma and in different neurodegenerative disorders, including AD

and Parkinson's disease (Heneka et al., 2014; McCoy and Tansey, 2008; Wyss-Coray and Mucke, 2002). Elevated TNF-α has further been linked to cognitive deficits (Azevedo et al., 2013; Lourenco et al., 2013). In peripheral tissues and hypothalamic cells, is suggested that palmitate activates Toll-like receptors 2/4 leading to increased inflammatory response, insulin resistance and cellular stress (Holland et al., 2011; Shi et al., 2006).

In conclusion, current findings indicate that palmitate levels are increased in the CSF of overweight and obese humans. In mice, palmitate induces hippocampal inflammation, and triggers increased TNF-α levels, inhibition of synaptic plasticity and memory impairment. Collectively, results suggest a mechanism by which excess palmitate derived from unhealthy diets affects brain function and contributes to cognitive impairment in obese and T2D patients. Further, strategies aimed at decreasing brain inflammation in obesity and T2D may help to alleviate the impact of palmitate in the brain. A healthy lifestyle that prevents excessive weight gain may prevent the increase in SFAs in the circulation and in the brain, thus contributing to healthy brain aging.

**Acknowledgments**

This work was supported by grants from Human Frontiers Science Program (HFSP) and John Simon Guggenheim Foundation (to F.G.D.F.), National Institute for Translational Neuroscience (INNT/Brazil), the Brazilian funding agencies Conselho Nacional de Desenvolvimento Científico e Tecnológico (CNPq) and Fundação de Amparo à Pesquisa do Estado do Rio de Janeiro (FAPERJ) (to S.T.F. and F.G.D.F). H.M.M, G.S.S.S, B.C.M, J.R.C, V.S.M.C., G.C.K., J.T.S.F and J.H.L were supported by CNPq and FAPERJ predoctoral and

postdoctoral fellowships. This work has been partially developed and supported through the LABEX (excellence laboratory, program investment for the future) DISTALZ (Development of Innovative Strategies for a Transdisciplinary approach to ALZheimer's disease) and the Hospital University Federation (FHU) OncoAge (FC). We thank Ana Claudia Rangel and Mariângela Viana for administrative and technical support. We thank Dr. Wagner Seixas (Federal University of Rio de Janeiro, Brazil) for insightful discussions and technical advice.

**Author Contributions:** Conceptualization, F.G.D.F and H.M.M; Methodology, F.G.D.F., S.T.F. and H.M.M; Investigation, H.M.M, G.S.S.S., M.R.S., C.V.L.T, J.R.C, V.S.M.C., B.C.M, J.T.S.F, L.F.G., J.H.L., M.S.O., R.P.P. and C.P.F.; Resources, J.M.D.G., A.G., L.A.V., F.C., M.L.B., D.E.C., S.T.F and F.G.D.F.; Writing – Original Draft, F.G.D.F., S.T.F. and H.M.M, with input from authors; Writing – Review & Editing, F.G.D.F., S.T.F. and H.M.M., Supervision, F.G.D.F.; Funding Acquisition, F.G.D.F. and S.T.F.

## Declaration of Interests

The authors declare no competing interests.

## Figure Legends

**Figure 1. CSF palmitic acid is increased in overweight and obese individuals, correlates with BMI and abdominal circumference, and inversely correlates with MMSE scores in overweight subjects with diabetes, hypertension and dyslipidemia. See also Figure S1 and Table S1.**

**(A)** CSF palmitic acid in normal weight (N = 14), overweight (N = 26) and obese (N= 9) subjects (classified by BMI). ****$p < 0.0001$ (one-way ANOVA followed by Holm-Sidak's *post hoc* test).

**(B)** Correlation between CSF palmitic acid and BMI in normal weight (green), overweight (blue) and obese (orange) subjects; linear regression, $r^2$ and p values as indicated.

**(C)** Correlation between CSF palmitic acid and abdominal circumference in normal weight (green), overweight (blue) and obese (orange) subjects (classified by BMI); linear regression, $r^2$ and p values as indicated.

**(D)** CSF palmitic acid in overweight subjects according to absence (N = 11) or presence (N = 15) of diabetes, hypertension or dyslipidemia. p = 0.09 (unpaired t-test).

**(E)** Inverse correlation between CSF palmitic acid and MMSE score in overweight subjects with diabetes, hypertension or dyslipidemia (linear regression, $r^2$ and p values as indicated).

**(F)** Lack of correlation between CSF palmitic acid and MMSE score in overweight subjects without diabetes, hypertension or dyslipidemia (linear regression, $r^2$ and p values as indicated).

**Figure 2. Palmitate inhibits long term potentiation and induces memory impairment in mice. See also Figure S2 and Figure S3.**

**(A-C)** Long-term potentiation (LTP) was induced by high-frequency stimulation (HFS, arrow) at the CA3 hippocampal subregion and recording in CA1 in awake freely-moving male 3-5-month-old mice, 10 days after intrahippocampal infusion of vehicle or palmitate (0.3 nmol). N = 6 vehicle-infused/N=8 palmitate-infused mice.

**(A)** Measurements performed immediately following HFS.

**(B)** Averaged fEPSP of the time points from 20 minutes to 30 minutes after HFS. Bars represent means (± SEM). **** $p < 0.0001$ (unpaired t-test).

**(C)** Measurements performed on subsequent days following LTP induction. *$p < 0.05$ (two-way ANOVA followed by Holm-Sidak's *post hoc* test).

**(D)** Novel object recognition (NOR) memory in male 3-5-month-old mice that received an i.c.v. infusion of vehicle or palmitate (3 nmol) 10 days before testing. Bars represent means (± SEM) exploration times for familiar (F) and novel (N) objects. Symbols represent individual animals. ***$p < 0.0005$ (unpaired t-test).

**(E)** Novel object location (NOL) memory in male 3-5-month-old mice that received an i.c.v. infusion of vehicle or palmitate (3 nmol) 10 days before testing. Bars represent means (± SEM) exploration times for objects in the original location (O) or novel location (N). Symbols represent individual animals. ****$p < 0.0001$ (unpaired t-test).

**(F)** Latency to step down in the step-down inhibitory avoidance task of male 3-5-month-old mice 10 days after i.c.v. infusion of vehicle or palmitate (3 nmol). Bars represent medians with interquartile range and symbols represent individual animals. **$p < 0.005$ (Mann-Whitney test).

**(G)** Primary latency time in the training phase of the Barnes maze for vehicle- or palmitate infused 3-5-month-old male mice. Symbols represent means ± standard errors. N = 7 vehicle-infused/6 palmitate-infused mice. **p = 0.005 (two-way ANOVA followed by Sidak's *post hoc* test).

**(H)** Primary errors in the training phase of the Barnes maze for vehicle- or palmitate infused 3-5-month-old male mice. Symbols represent means ± standard errors. N = 7 vehicle-infused/6 palmitate-infused mice. p = 0.09 (two-way ANOVA followed by Sidak's *post hoc* test).

**(I)** Time in target zone on test day 5 in the Barnes maze for vehicle- or palmitate-infused 3-5-month-old male mice. Bars represent means ± standard errors, and symbols represent individual mice. N = 7 vehicle-infused/6 palmitate-infused mice. **p < 0.005 (unpaired t-test).

**Figure 3. Palmitate reduces insulin expression and impairs IRS-1 signaling in hippocampal neurons. See also Figure S4.**

**(A)** Relative insulin expression (mRNA) in cultured hippocampal cells exposed to vehicle or 200 μM palmitate for 24 hours. Bars represent means ± standard errors and symbols represent independent cultures. **p < 0.005 (paired t-test).

**(B-I)** Neuronal IRS-1pTyr612 (B-C), pSer636 (D-E), pSer307 (E-F) and pSer312 (G-H) immunoreactivities in cultured hippocampal neurons exposed to vehicle or 200 μM palmitate for 4 hours (10-30 images analyzed per experimental condition per experiment using independent neuronal cultures). Scale bar = 10 μm. Bars represent means ± standard errors and symbols represent independent cultures. *p < 0.05 (unpaired t-test). In representative IRS-1 PTyr612 images, for better viewing, the image color was changed to green using ZEN software.

**Figure 4. Palmitate increases GFAP and Iba-1 immunoreactivities *in vitro* and *in vivo*.**

**(A)** Representative images of GFAP immunolabeling in hippocampal cultures exposed to vehicle or 200 μM palmitate for 4 hours (10-15 images analyzed per experimental condition per experiment using independent hippocampal cultures). Scale bar = 10 μm.

**(B)** GFAP immunoreactivity in hippocampal cultures. Bars represent means ± standard errors and symbols represent independent cultures. **p = 0.008 (unpaired t-test).

**(C, D)** Representative images of GFAP immunolabeling in the dentate gyrus of the hippocampus from 2-4-month-old mice that received i.c.v. infusions of vehicle or palmitate (3 nmol). Animals were perfused 10 days after palmitate infusion. Scale bar = 50 μm; 10 μm (inset). **(D)** Bars represent means ± standard errors and symbols represent individual animals. * p < 0.05 (unpaired t-test).

**(E)** Representative images of Iba-1 immunolabeling in purified microglial cultures exposed to vehicle or 200 μM palmitate for 2 hours (10-25 images analyzed per experimental condition per experiment with independent microglial cultures). Scale bar = 10 μm.

**(F,G)** Iba-1 immunoreactivity **(F)** and cell area **(G)** in purified microglial cultures exposed to vehicle or palmitate. Bars represent means ± standard errors and symbols represent independent cultures. *$p < 0.05$; **$p < 0.005$ (unpaired t-test).

**(H,I)** Representative images of Iba-1 immunolabeling **(H)** and number of Iba-1 positive cells **(I)** in the dentate gyrus of the hippocampus from 2-4 month-old mice that received i.c.v. infusions of vehicle or palmitate (3 nmol). Animals were perfused 10 days after palmitate infusion. Scale bar = 50 μm; 10 μm (inset). (**I**) Bars represent means ± standard errors and symbols represent individual animals. **$p < 0.005$ (unpaired t-test).

**Figure 5. Microglial activation mediates inhibition of neuronal IRS-1 signaling and memory impairment by palmitate.**

**(A**) Representative images of Iba-1 immunolabeling in purified microglial cultures exposed to vehicle or 200 μM palmitate for 2 hours in the absence or presence of 1 μM minocycline (10-25 images analyzed per experimental condition per experiment with independent microglial cultures). Scale bar = 10 μm.

**(B, C)** Iba-1 immunoreactivity **(B)** and cell area **(C)** in purified microglial cultures exposed to vehicle or palmitate, in the absence or presence of minocycline. Bars represent means ± standard errors and symbols represent independent cultures. *$p < 0.05$ (two-way ANOVA followed by Holm-Sidak's post hoc test). Vehicle and palmitate conditions were showed in Figure 4 F,G.

**(D, E)** Neuronal IRS-1pSer636 immunoreactivities in hippocampal cultures exposed for 4 hours to conditioned medium from purified microglial cultures treated with vehicle or 200 μM palmitate (10-30 images analyzed per experimental condition per experiment using independent hippocampal and microglial cultures). Scale bar = 10 μm. Bars represent means ± standard errors and symbols represent experiments with independent hippocampal and microglial cultures. *$p < 0.05$ (unpaired t-test).

**(F, G)** Neuronal IRS-1pSer636 immunoreactivities in hippocampal cultures exposed for 4 hours to vehicle or 200 μM palmitate in the absence or presence of 1 μM minocycline (10-30 images analyzed per experimental condition per experiment using independent cultures). Scale bar = 50 μm; 10 μm (inset). Bars represent means ± standard errors and symbols represent experiments from 3 independent cultures. *$p < 0.05$; **$p < 0.005$ (two-way ANOVA followed by Holm-Sidak's post hoc test).

**(H)** Novel object recognition (NOR) test in male 3-5-month-old mice infused i.c.v. with vehicle or palmitate (3 nmol) and treated or not with minocycline (50 mg/kg/d, ip, for 3 consecutive days ending on the day of vehicle or palmitate infusion). Testing was performed 10 days after infusions. Bars (means ± SEM) represent time spent exploring the familiar (F)

or novel (N) objects, and symbols represent individual mice. *p < 0.05; **p =0.005; ***p < 0.001 (two-way ANOVA followed by Holm-Sidak's post hoc test).

**(I, J)** Representative images of Iba-1 immunolabeling **(I)** and number of Iba-1 positive cells **(J)** in the dentate gyrus of the hippocampus from 2-4 month-old mice that received i.c.v. infusions of vehicle or palmitate (3 nmol) and were treated or not with minocycline (50 mg/kg/d, IP, for 3 consecutive days ending on the day of vehicle or palmitate infusion). Animals were perfused 10 days after palmitate infusion. Scale bar = 50 μm; 10 μm (inset). (**J**) Bars represent means ± standard errors and symbols represent individual animals. **p < 0.005 (two-way ANOVA followed by Dunnett's post hoc test). Part of the vehicle and palmitate data was shown in Figure 4I.

**Figure 6. Increased hippocampal TNF-α expression mediates neuronal IRS-1 signaling impairment *in vitro* and memory deficits induced by palmitate.**

**(A)** TNF-α released to the culture medium in hippocampal cultures exposed to vehicle or 200 μM palmitate for 4 hours. Symbols represent paired conditions per culture. N= 8 independent cultures. **p = 0.006 (paired t-test).

**(B-E)** TNF-α mRNA **(B, D)** and protein levels (**C, E**) in the hippocampi of 3-5-month-old mice infused i.c.v. with vehicle or palmitate (3 nmol) 24 hours (**B, C**) or 10 days (**D, E**) prior to collection of hippocampi. Bars represent means ± standard errors and symbols represent individual animals. *p < 0.05 (unpaired t-test).

**(F, G)** Neuronal IRS-1pSer636 immunolabeling in hippocampal cultures exposed for 4 hours to vehicle or 200 μM palmitate in the absence or presence of 1 μg/ml infliximab (20-30 images analyzed per experimental condition per experiment using independent cultures). Scale bar = 10 μm. Bars represent means ± SEM and symbols represent independent cultures. **p < 0.005; *p < 0.05 (two-way ANOVA followed by Holm-Sidak's post hoc test).

**(H, I)** Novel object recognition (NOR) test in male 3-5-month-old mice infused i.c.v. with vehicle or palmitate (3 nmol) and treated or not with infliximab (100 ng, i.c.v., 30 min previously to the infusion of vehicle or palmitate). Testing was performed 24 hours (**H**) or 10 days (**I**) after infusions. Bars (means ± SEM) represent time spent exploring the familiar (F) or novel (N) objects, and symbols represent individual mice. *p < 0.05, **p =0.005 (two-way ANOVA followed by Holm-Sidak's post hoc test).

**(J, K)** Representative images of Iba-1 immunolabeling **(J)** and number of Iba-1 positive cells **(K)** in the dentate gyrus of the hippocampus from 2-4 month-old mice that received i.c.v. infusions of vehicle or palmitate (3 nmol) and were treated or not with infliximab (100 ng, i.c.v., 30 min previously to the infusion of vehicle or palmitate). Animals were perfused 10 days after palmitate infusion. Scale bar = 50 μm; 10 μm (inset). (**K**) Bars represent means ± standard errors and symbols represent individual animals. **p < 0.005 (two-way ANOVA followed by Dunnett's post hoc test). Part of the vehicle and palmitate data was shown in Figure 4I.

**Figure 7. Infliximab prevents memory deficits in HFD mice and genetic deletion of TNFR1 prevents memory impairment induced by palmitate.**

**(A)** Novel object recognition (NOR) test in male 6-7-month-old mice fed normal diet (ND) or high fat diet (HFD) for 12 weeks. Bars (means ± SE) represent time spent exploring the familiar (F) or novel (N) objects, and symbols represent individual animals. *p < 0.05 (unpaired t-test).

**(B)** Novel object recognition (NOR) test in male 6-7-month-old mice fed high fat diet (HFD) for 16 weeks and treated or not with infliximab (10 μg, i.c.v., for 3 days before memory task). Bars (means ± SE) represent time spent exploring the familiar (F) or novel (N) objects, and symbols represent individual animals. *p < 0.05 (unpaired t-test).

**(C, D)** Novel object recognition (NOR) test in 3-5month-old wild type or $TNFR1^{-/-}$ mice infused i.c.v. with vehicle or palmitate (9 nmol). Testing was performed 24 hours (**C**) or 8 days (**D**) after infusions. Bars (means ± SEM) represent time spent exploring the familiar (F) or novel (N) objects, and symbols represent individual animals. *p < 0.05, **p < 0.005, ***p < 0.0005, ****p < 0.0001 (two-way ANOVA followed by Holm-Sidak's post hoc test).

## STAR Methods

### CONTACT FOR REAGENT AND RESOURCE SHARING

This study did not generate new unique reagents. Further information and requests for resources and reagents should be directed to and will be fulfilled by the Lead Contact, Fernanda G. De Felice (felice@bioqmed.ufrj.br).

### EXPERIMENTAL MODEL AND SUBJECT DETAILS

*Human subjects:* We studied 49 subjects diagnosed as aMCI recruited from the Neuropsychology and Dementia clinic, Hospital de Clínicas, University of Campinas invited to participate in the project in order to check their memory (Magalhães et al., 2018; Rabelo et al., 2017; Teixeira et al., 2016, 2018; Weiler et al., 2017). aMCI patients were diagnosed using the core criteria of the National Institute on Aging/Alzheimer's Association for MCI (Albert et al., 2011; Raj et al., 2012) and had a score of 0.5 (with an obligatory memory score of 0.5), estimated on the basis of a semi structured interview. Exclusion criteria for all participants were history of other neurologic/psychiatric diseases or head injury with loss of

consciousness, drug or alcohol addiction, a Hachinski ischemic score 15 above 4 and a Fazekas Scale score16 above 1. The Medical Research Ethics Committee of the University of Campinas (UNICAMP) approved our study, and we obtained written informed consent from all participants (or from their responsible guardians if the participants were incapable of consenting) before study initiation. Pre-diagnostic procedures also comprised of laboratory tests including vitamin B12, folate, and thyroid hormones. CSF was obtained from all participants once, by lumbar puncture of the L3/L4 or L4/L5 intervertebral space, using a 25-gauge needle, and collected via a syringe in 12-mL polypropylene tubes (Sarstedt, Nümbrecht, Germany). CSF samples were centrifuged at 700 rpm for 10 minutes at 4ºC and were subsequently aliquoted into 1 ml microtubes (Eppendorf) and stored at -80ºC until the time of analysis.

BMI was calculated by dividing the person´s weight, in kilograms, by their height, in meters squared, or BMI = weight (in kg)/ height$^2$ (in m$^2$). BMI was categorized as: normal weight: 18.5-23.9 kg/m$^2$; overweight: 24.0-27.9 Kg/m$^2$; and obesity: ≥ 28 kg/m$^2$. Abdominal circumference was measured to the nearest 0.1 cm by a non-elastic flexible tape. We used the method recommended by the World Health Organization (WHO), which consists measuring midway between the lowest rib margin and the iliac crest at the mid-axillary line World Health Organization (WHO Consultation on Obesity, 1999; Geneva, Switzerland) Abdominal obesity was defined as >102cm cm for men and > 88 cm for women (Garvey et al., 2016).

Patients were divided into groups with or without diabetes, dyslipidemia and hypertension based on the use of medication for these diseases.

*Intrahippocampal palmitate administration and placement of recording electrodes:* All experiments were conducted in accordance with the "Principles of Laboratory Animal Care" (NIH publication no. 85–23, revised 1996) and with the Guidelines of the European Union (2003/65/CE) for the use of laboratory animals in chronic experiments. Every effort was made to reduce the number of animals used and to minimize their suffering.
C57BL/6 male mice (3-5 months-old; 25-35g) were obtained from an official supplier (University of Granada Animal House, Granada, Spain) and housed five per cage until

experiments began. Mice were kept on a 12 h light/dark cycle with constant ambient temperature (21.5 ± 1.5 °C) and humidity (55 ± 8%). Food and water were available ad libitum. Mice were anesthetized with 4% chloral hydrate and, prior to electrode implantation, received a single intra-CA2 (1.8 mm lateral, 1.5 mm posterior do bregma and 1.1 mm from the brain surface; Franklin and Paxinos, 2004) infusion of palmitate (0.3 nmol) or vehicle in a final volume of 1 μL using a Hamilton syringe, which was kept in place for an additional 30 seconds after drug administration to avoid backflow. Immediately after infusion, bipolar stimulating electrodes were implanted in the CA3 hippocampal subregion of the dorsal hippocampus (2 mm lateral and 1.5 mm posterior to bregma, and 1–1.5 mm from the brain surface; Franklin and Paxinos, 2004) and a bipolar recording electrode was placed in the ipsilateral *stratum radiatum* underneath the CA1 area (1.2 mm lateral and 2.2 mm posterior to bregma and 1–1.5 mm from the brain surface; Franklin and Paxinos, 2004). Electrodes were made from 50-μm Teflon-coated tungsten wire (Advent Research Materials, UK). The final location of the recording electrodes in the CA1 area was determined after the field potential depth profile evoked by paired (10- to 500-ms interval) pulses presented to the Schaffer collateral. A bare silver wire was fixed to the skull as ground. The four wires were soldered to a four-pin socket (RS Amidata) that was then fixed to the skull using dental cement (Gruart et al., 2006; Madronal et al., 2007). After surgery, animals were housed in individual cages until the end of experiment. Only data from animals with correct electrode placement were analyzed.

*Intracerebroventricular infusion of palmitate or oleate in Swiss mice:* Male Swiss mice were obtained from our animal facility (Federal University of Rio de Janeiro) or from Laboratory Animal Breeding Center (Fundação Oswaldo Cruz – CECAL/Fiocruz, Rio de Janeiro) and were 2-5 months-old at the beginning of experiments. Animals were housed in groups of five per cage with free access to food and water, under a 12 h light/dark cycle with controlled room temperature (21 ± 2 °C). The animals weighed approximately 30 – 50 g. Mice were randomly assigned into one of two groups: vehicle or palmitate.

For intracerebroventricular (i.c.v.) infusion of vehicle or palmitate, animals were anesthetized and carefully restrained with 2.5% isoflurane (Cristalia) using a vaporizer system, and a 2.5-mm-long needle was unilaterally inserted 1 mm to the right of the midline

point equidistant from each eye and 1 mm posterior to a line drawn through the anterior base of the eyes (Clarke et al., 2015; Figueiredo et al., 2013; Laursen SE, 1986; Lourenco et al., 2013). Three nmol of palmitate or oleate (or an equivalent volume of vehicle) were infused in a final volume of 3 µl. When indicated (see Results and Figure legends), one hour before i.c.v. palmitate infusion mice received 10 ng infliximab (or an equivalent volume of phosphate buffered saline - PBS) in a final volume of 1 µl at the same injection site as the fatty acid. In these animals, 3 nmol palmitate (or an equivalent volume of vehicle) were infused in a final volume of 2 µl so that the final volume injected i.c.v. was 3 µl.

Regarding the LTP experiment, we increased the amount injected palmitate in the behavioral experiments to ensure its distribution to different brain regions following icv infusion.

Accurate placement of the needle into the right lateral ventricle was confirmed by macroscopic examination of dissected brains before biochemical analysis. Mice showing any signs of misplaced injections or brain hemorrhage were excluded from further analysis (~ 5% of animals throughout our study). All procedures were performed in the light phase of the daily cycle, followed the "Principles of Laboratory Animal Care" (US National Institutes of Health) and were approved by the Institutional Animal Care and Use Committee of the Federal University of Rio de Janeiro (protocols IBQM045 and IBQM133/15).

*Intracerebroventricular infusion of palmitate in TNFR1$^{-/-}$ and C57BL/6 mice:* Male 3-4 months-old TNFRp55$^{-/-}$ (TNFR1 KO) mice (Arruda et al., 2011; Pfeffer et al., 1993) were kindly donated by Dr. Licio A. Velloso from the University of Campinas, São Paulo, Brazil, and male 3-4 months-old C57BL/6 wild type mice from our animal facility (Federal University of Rio de Janeiro) were used as controls. The animals weighed approximately 25-35 g. All animals were housed in groups of five per cage with free access to food and water, under a 12 h light/dark cycle with controlled room temperature (21 ± 2 °C) and were randomly assigned into vehicle or palmitate groups. All procedures were performed in the light phase and followed the "Principles of Laboratory Animal Care" (US National Institutes of Health) and were approved by the Institutional Animal Care and Use Committee of the Federal University of Rio de Janeiro (protocol # IBQM133/15).

TNFR1$^{-/-}$ and controls were randomly assigned into one of two groups: vehicle or palmitate. Intracerebroventricular infusion of vehicle or palmitate were performed as described above.

Nine nmol palmitate (or an equivalent volume of vehicle) were infused in a final volume of 1.5 µl. We increased the amount injected palmitate in the behavioral experiments to ensure its distribution to different brain regions following i.c.v. infusion.

*High fat diet (HFD) administration:* Male 3-3.5 months-old C57BL/6 wild type from our animal facility (Federal University of Rio de Janeiro) were randomly divided into two groups fed either standard rodent chow or HFD (35% fat content by weight - PragSoluções®; Razolli *et al.*, 2015) for 16 weeks. For NOR experiments, HFD mice were treated with infliximab (10 µg) or PBS for 3 days before memory testing, with the last injection in the day of NOR task. Animals were housed in groups of five per cage with free access to food and water, under a 12 h light/dark cycle with controlled room temperature (21 ± 2 °C). All procedures were performed in the light phase and followed the "Principles of Laboratory Animal Care" (US National Institutes of Health) and were approved by the Institutional Animal Care and Use Committee of the Federal University of Rio de Janeiro (protocol # IBQM133/15).

*Mature hippocampal cultures:* Primary rat hippocampal cultures were prepared according to established procedures (De Felice et al., 2009) and adapted from the original protocol described by Brewer (Brewer, 1997). Hippocampi from 18-day-old embryos were dissected and the meninges were removed. Tissue was dissociated in PBS 0.05% trypsin/EDTA (Invitrogen) solution at 37 °C for 5-10 minutes under occasional gentle shaking followed by mechanical dissociation with glass Pasteur pipettes in Dulbecco's Modified Eagle Medium (DMEM) (Gibco) medium supplemented with 10% horse-serum (Invitrogen) and antibiotics (100 U/ml penicillin/streptomycin) (Invitrogen). Cells in suspension were counted in a Neubauer chamber and were plated on culture plaques or glass coverslips previously coated with 10 µg/ml or 1 mg/ml poly-L-lysine, respectively. The density of culture was 50.000 cells/well (260 cells/mm$^2$) on coverslips for immunocytochemistry experiments and 30.000 cells/well (645 cells/mm$^2$) for the cell viability experiments. Cells were maintained at 37 °C in a humidified atmosphere containing 5% $CO_2$ for 60 minutes and DMEM was replaced by Neurobasal medium supplemented with 2% B27 supplement (Invitrogen), 0.5 mM Glutamax (Invitrogen), 100 U/ml penicillin/streptomycin (Invitrogen) and 10 µg/ml amphotericin-B (Invitrogen). Cultures were maintained at 37 °C in a humidified atmosphere containing 5%

$CO_2$ for 18-21 days prior to use. Our cultures contain, on average, 50% neurons and 50% non-neuronal cells. The objective is to have a mixed culture to investigate the interplay between neuronal and non-neuronal cells. Sex of 18-day-old embryos could not be determined at this embryonic age and the embryos were not weighed.
Cultures were exposed at 37 °C to 50-500 μM palmitate for 4, 24 or 48 hours. When present, infliximab (1 μg/ml) or minocycline (1 μM) were added to cultures 30 minutes or 1 hour before application of vehicle or palmitate (200 μM), respectively.

*Primary cultures and conditioned media from mouse microglia:* Primary microglial cultures were prepared as described previously (Azevedo et al., 2013; Ledo et al., 2013, 2016). Cortices from neonatal Swiss mice were dissociated, and the resulting cells were plated on poly-L-lysine-coated 75-$cm^2$ flasks. The cells were maintained in DMEM with F12 medium (1:1 ratio), 10% fetal bovine serum (FBS) and 1% penicillin/streptomycin for 2 weeks at 37 °C in a humidified atmosphere containing 5% $CO_2$. The medium was changed after 1 week and before cell harvesting. After 14 days, microglia were harvested using an orbital shaker. The cells were counted and plated in 24-well plates for assays. Microglial cells were exposed at 37 °C to 200 μM palmitate, 200 μM oleate or vehicle for 2 hours. E. coli lipopolysaccharide (LPS, 100 ng/ml) was used as a positive control for microglial activation. When present, minocycline (1 μM) were added to cultures 1 hour before application of vehicle or palmitate (200 μM), respectively.
For experiments using conditioned medium, cells were washed 2 times with warm DMEM with F12 medium and changed to Neurobasal medium overnight to obtain conditioned medium. The conditioned medium was then incubated with hippocampal cultures for 4 hours.

**METHOD DETAILS**

*Palmitic acid measurements by GC-MS*: For fatty acid profile determination, 170 μL cerebrospinal fluid were taken in a screw cap glass tube containing 25 μg internal standard (tridecanoic acid - C13:0). Thereafter, 1 mL of 0.5 M NaOH-methanol was added and the

sample was boiled at 100 °C for 15 min. After cooling the samples, 2 mL of BF3-methanol was added and the sample was boiled at 100 °C for 20 s. The sample was again cooled to room temperature and 1 mL of isooctane was added. The tubes were shaken and 5 mL of saturated NaCl solution was added. After phase separation, the supernatant was collected and evaporated with the aid of nitrogen gas to concentrate the fatty acid methyl esters (FAME). FAME were resuspended in 50 µL hexane for chromatographic analysis (Shirai et al., 2005). Chromatographic analyses were performed using a gas chromatograph-mass spectrometer (model GCMS-QP2010 Ultra; Shimadzu). A fused silica capillary column Stabilwax (length, 30 m; internal diameter, 0.25 mm; thickness, 0.25 µm; Restek, USA) was used to inject 1 µL of the sample at 250 ºC. High-grade pure helium (He) was used as the carrier gas with a constant flow rate of 1.3 mL/min with a split injection of 2:1. The oven temperature was programmed from 80 to 175 °C at a rate of 5 °C/min, followed by another gradient of 3 °C/min to 230 °C, which was maintained for 10 min. Mass conditions were as follows: ionization voltage, 70 eV; ion source temperature, 200 ºC; full scan mode in the 35–500 mass range with 0.2 s/scan velocity.

*Palmitate and oleate preparation:* The protocol for preparation of palmitate and oleate solutions was adapted from the protocol described by Mayer and Belsham (Mayer and Belsham, 2010). Solutions for i.c.v. infusions in mice were prepared from a stock solution of 100 mM sodium palmitate (Sigma) or sodium oleate (Sigma) solubilized in methanol (Tedia). Palmitate or oleate were solubilized in methanol under occasional shaking at 60 ° C (palmitate) or at room temperature (oleate). The stock solution was then diluted in Neurobasal culture medium (Gibco) containing 5% fatty acid free albumin (Sigma) for 1 hour at 37 ° C and shaking. After this period, the solutions were used for icv infusions. For Swiss mice, 2 or 3 µl of the final infused solution contained 3 nmol of fatty acids. For C57BL/6 and TNFR1$^{-/-}$mice, 1.5 µl of final infused solution contained 9 nmol of palmitate. Vehicle was Neurobasal medium with 5% fatty acid free albumin plus the corresponding volume of methanol. The methanol in the final solution was a very low volume, with only one residual of the solvent remaining (0,015 - 0,03%).

For primary hippocampal cultures, 5 mM palmitate solution in Neurobasal culture medium with 5% fatty acid free albumin was diluted to 50-500 μM in culture medium. The vehicle was Neurobasal with 5% fatty acid free albumin plus the corresponding volume of methanol. The BSA solution was filtered through sterile 0.22 μm filter before palmitate or oleate dilution, and all solutions were performed sterile in a laminar flow hood. Furthermore, the pH of the solutions was measured after preparation, and was in the range of 7.2-7.4.
The amount of palmitate used in our studies in mice (3 or 9 nmol) corresponds to 22 or 66 μg/ml CSF, respectively (assuming uniform distribution in 35 μl of CSF). These concentrations are ~ 3.5-10-fold higher than we found in the CSF of obese subjects, and were chosen to allow investigation of the impact of palmitate in mice within a reasonable experimental timeframe.

*Long term potentiation (LTP):* Recordings took place 10 days after electrode implantation in alert behaving mice. Field excitatory post-synaptic potential (fEPSP) baseline values were recorded using 100 μs, square, biphasic paired pulses for 15 min before LTP induction. For construction of I/O curves, stimulus intensities ranged from 0.02mA to 0.4mA and were elicited at a 40ms interstimulus interval. The stimulus intensity was set at ~35% of the intensity necessary for evoking a maximum fEPSP response (i.e., well bellow the threshold for evoking a population spike). For LTP induction, a HFS protocol consisting of five 200 Hz, 100 ms-long trains of pulses at a rate of one per second was used. This protocol was applied six times, at intervals of 1 min. After HFS presentation, recordings of double-pulse stimulation at Schaffer collaterals were conducted for another 20 min to evaluate whether the LTP protocol was effective. During the following three days, mice were submitted to 15 min-long daily recording sessions to assess the persistence of LTP. According to previous studies (Gruart et al., 2006; Madronal et al., 2007), this HFS was enough to evoke a saturating LTP response, lasting 3 days, without the appearance of abnormal spikes in EEG recordings and/or any noticeable epileptic seizure.
All data were stored digitally on a computer through an analog/digital converter (1401 Plus; CED), at a sampling frequency of 11–22 kHz and with an amplitude resolution of 12 bits. Evoked fEPSPs amplitudes were analyzed with the help of commercial software (Spike 2

and GraphPad Prism 7) and data are expressed as average amplitude of fEPSP for every 2 min of recording. Statistical analysis for each analysis is described in the corresponding Figure Legends.

*Novel object recognition (NOR) and novel object location (NOL) tests*: Tests were performed in a 30 (w) x 30 (d) x 45 (h) cm arena. Before training, each animal was submitted to a 5 min habituation session, in which they were allowed to freely explore the empty arena. Training consisted of a 5 min session during which animals were placed at the center of the arena in the presence of two identical objects and the time spent exploring each object was recorded by a trained researcher. Sniffing and touching the object were considered as exploratory behavior. Approximately one to two hours after training, animals were again placed in the arena for the test session, when one of the two objects used in the training session was replaced by a new one in NOR paradigm or moved to a new location in NOL paradigm, and the time spent exploring familiar and novel objects (or object at the novel location) was measured. The arena and objects were cleaned thoroughly between trials with 40% ethanol to eliminate olfactory cues. Test objects were made of plastic (approximately 3 cm (w) x 3 cm (d) x 4cm (h)) and during behavioral sessions were fixed to the arena floor using tape to prevent displacement caused by exploratory activity of the animals. Preliminary tests showed that none of the objects used in our experiments evoked innate preference by animals, i.e., during the training period, mice explored each object approximately 50% of the time. NOR test in C57BL/6 mice was performed without the habituation phase. In the training phase, the animals explored approximately 45 - 55% of the total time each o object. Results were expressed as percentage of time exploring each object or location (familiar or novel) in relation a total exploration time during the test session, and statistical analysis for each experiment is described in the corresponding Figure Legends.

*Step-down inhibitory avoidance test:* The test was carried out in an aluminum and acrylic box measuring 200 mm x 75 mm, a floor consisting of a grid of steel bars with a spacing of 12.5 mm (Insight EP 104R) and an adapted platform of 2 cm of height placed in the center of the grid. In the training phase, each animal was gently placed on the platform. When the animal stepped down from the platform onto the grid with the 4 paws, they received a 0.7

mA footshock (stimulus) for 2 seconds. The animal was then withdrawn from the apparatus. After 24h (test session), each animal was placed on the platform again. In this session, no shock was applied when the animal stepped-down on the grid. After stepping down, each animal was withdrawn from the apparatus and placed back in the home cage. The time in platform before stepping down on the grid (latency) was measured during the training and test sessions with a manual chronometer by a trained researcher. Step-down latencies were cut-off at 300 s in the training and test sessions, and animals that did not step down during 300 seconds were excluded from analysis. Results are represented as median and interquartile range of the latency to step down in the test session and the difference was considered statistically if $p < 0.05$ (Mann-Whitney test).

*Barnes maze test:* The Barnes maze protocol was adapted from (Sunyer et al., 2014). The maze consists of a white circular platform (92 cm of diameter) elevated 105 cm above the ground with 20 equally spaced holes (5 cm diameter, 7.5 cm between holes) along the perimeter with a darkened escape box in a constant position under one of the holes at the edge of the platform. Mice are expected to learn the location of the escape hole using extra-maze visual cues including geometric shapes (triangle, rectangle and circle) placed on the walls of the room.

To familiarize mice with the maze and the existence of the escape box, they were subjected to one habituation trial in the first day prior to the initial trial. This habituation consisted of placing the animal in a cylindrical chamber in the middle of the maze and after 10 seconds, the chamber was removed, and the mouse was gently guided to the escape hole, where it remained for 2 minutes.

In the next step, acquisition training was performed with four trials per day for four days. For each trial, mice were placed in the cylindrical chamber in the middle of the maze and, after 10 seconds, the chamber was removed, and mice were allowed to explore the maze for 3 minutes. The trial ended when the animal entered the escape hole or after 3 minutes. If a mouse did not enter the escape hole within 3 minutes, the animal was gently guided to it and kept inside the box for 1 minute. Mice were returned to their home cages until the next trial, with a 15-minute interval between trials. Time (primary latency) and number of errors (primary errors) to reach the escape hole for the first time were measured. Head deflections

into incorrect holes of the maze were considered errors and were counted by the experimenter.

On day 5, mice underwent the probe trial to access reference memory (short-term memory retention) in which the escape hole was closed. Mice were placed in the cylindrical chamber in the middle of the maze. After 10 seconds, the chamber was removed, and mice were allowed to explore the maze for 90 seconds. The amount of time that animals spent in the escape hole quadrant was recorded. In all experimental steps, the maze was cleaned with 40% ethanol and air-dried before each trial and between mice. The platform was monitored using the ANY-maze software (Stoelting Co, IL, USA), which recorded the animal's position, total distance travelled and average speed. No differences in total distance travelled and average speed between vehicle or palmitate groups was observed. Importantly, there was no difference in average weights between vehicle- and palmitate-infused groups after i.c.v. infusion.

*Western blots*: Twenty-four hours or 10 days after i.c.v. infusion of palmitate, mice were euthanized by decapitation and the hippocampus was rapidly dissected and frozen in liquid nitrogen. For protein extraction, samples were thawed and homogenized in RIPA buffer (25 mM Tris–HCl, pH 7.5, 150 mM NaCl, 1% NP-40 (Invitrogen), 1% sodium deoxycholate, 0.1% SDS, 5 mM EDTA, 1% Triton X-100) containing a phosphatase and protease inhibitor cocktail (Pierce–Thermo Scientific, Rockford, IL). Protein concentration was determined using the BCA kit. Aliquots containing 50 μg protein were prepared in sample buffer containing 125 mM Tris-Cl, 10 % SDS, 0.05 % Bromophenol blue, 5% β-mercaptoethanol and 50% glycerol and resolved by SDS–PAGE in 10% polyacrylamide gels at 125 V. Proteins were electrotransferred to nitrocellulose for 1 h at 100 V. Membranes were blocked for 1 h with 3% bovine serum albumin in Tween-Tris buffer solution at room temperature or with Odyssey blocking buffer (Licor; Lincoln, NE; 1:2 dilution in Tween-Tris Buffer) and were incubated overnight at 2 °C with primary antibodies diluted in blocking buffer. Molecular weight markers (Benchmark pre-stained protein ladder; Life Technologies) were run in every gel. Primary antibodies used were: Synaptophysin (Abcam, Cat# ab8049; 1:1,000), cyclophilin B (Abcam, Cat# ab16045; 1:1,000), PSD-95 (Santa Cruz, Cat# SC 28491; 1:1,000) and β-actin (Abcam, Cat# ab6276; 1:10,000). After overnight incubation

with primary antibodies and washing with TBS-T, membranes were incubated with IRDye800CW- or IRDye680RD-conjugated secondary antibodies (Licor; 1:10,000) at room temperature for 1 h. Fluorescence intensities were detected in an Odyssey CLx apparatus (Licor). Scanned or digitized images were saved at high resolution (300 dpi) and bands were quantified by densitometry in Fiji software (Schindelin et al., 2012).

*RNA extraction and quantitative real-time PCR analysis*: Hippocampus from vehicle- or palmitate-infused mice or from cultured hippocampal cells were homogenized in 1 mL Trizol (Invitrogen) and RNA extraction was performed according to manufacturer's instructions. Purity and integrity of RNA were determined by the 260/280 nm and 260/230 absorbance ratio and by agarose gel electrophoresis. Only preparations with ratios >1.8 and no signs of RNA degradation were used. One µg RNA was used for cDNA synthesis using the Super-Strand III Reverse Transcriptase kit (Invitrogen) or High Capacity cDNA Reverse Transcription (Applied Biosystems). Expression of genes of interest was analyzed by qPCR on an Applied Biosystems 7500 RT–PCR system using the Power SYBR kit (Applied Biosystems). Actin was used as endogenous control. Primer pairs used are: rat ACTB (*forward*: AGTGTGACGTTGACATCCGTA; *reverse*: GCCAGAGCAGTAATCTCCTTCT), rat INS 2 (*forward*: CCTGCTCATCCTCTGGGAGC; *reverse*: TGTGCACCTTGTGGGTCCTCCA), mouse ACTB (*forward*: GCCCTGAGGCTCTTTTCCAG; *reverse*: TGCCACAGGATTCCATACCC), mouse INS2 (*forward*: ACATGGCCCTGTGGATGCGCT; reverse: CACGGCGGGACATGGGTGTG) and mouse TNF-α (*forward*: CCCTCACACTCAGATCATCTTCT; *reverse*: GCTACGACGTGGGCTACAG). Cycle threshold (Ct) values were used to calculate fold changes in gene expression using the $2^{-\Delta\Delta Ct}$ method. In all cases, reactions were performed in 15 µl reaction volumes.

*Immunocytochemistry and image analysis:* Hippocampal or microglial cultures were fixed by adding an equal volume of 4 % formaldehyde plus 4% sucrose (in PBS buffer) to the medium for 5 min followed by the removal of the entire fix/medium solution and replacement with 4 % formaldehyde for 10 min. Cells were rinsed 3 times with PBS, incubated with 10%

normal goat serum in PBS for 2 hours, permeabilized with 0.1 % Triton X-100 in PBS for 5 min and washed with PBS. Cells were then immunolabeled with primary antibodies (IRS-1 pTyr612, Sigma; 1:200 dilution; IRS-1 pS636, Santa Cruz; 1:200 dilution; IRS-1 pSer307, Invitrogen; 1:100 dilution; IRS-1 pSer312, Invitrogen; 1:100 dilution;; 1:100 dilution; Iba-1, Wako; 1:1,000 dilution and GFAP, Dako; 1:500 dilution) overnight at 4 °C. Cells were then rinsed three times with PBS and incubated for 2 h at room temperature with Alexa Fluor 594-conjugated anti-rabbit IgG secondary antibody or Alexa Fluor 555-conjugated anti-rabbit IgG secondary antibody (1:2,000 dilution; Molecular Probes, Inc., Eugene, OR) in PBS with 1% normal goat serum. Cells were rinsed four times with PBS and one time with deionized water, and coverslips were mounted with Prolong Gold mounting medium with DAPI (Molecular Probes). Images were obtained from randomly chosen fields (8-25 images per experimental condition, from one to three coverslips per condition, see "Figure Legends"), using a Nikon Digital Sight DS-Qi1Mc camera and Nikon Eclipse TE 2000-U fluorescence microscope or AxioCam MRm and Zeiss Axio Observer Z1 using 100× objective under conventional fluorescence microscope. Omission of primary antibodies eliminated all labeling.

Quantitative immunofluorescence data was measured in 8-bit grayscale photomicrographies and carried out by analysis of the fluorescence intensity at each pixel across the images using Fiji software (Schindelin, J. et al., 2012). The program analyzes a grayscale image by plots of the intensity of fluorescence at each pixel. An appropriate thresholding was employed to eliminate background signal in the images before analysis. Thus, the entire microscopic field imaged was included in analysis and the Raw Integrated Density (RawIntDens) is normalized by the number of DAPI positive cells. For conditions with two or three replicates, the mean of RawIntDens was calculated. The final result was expressed by the mean (± SEM) of RawIntDens / DAPI positive cells values of each independent experiment normalized by the mean of vehicle condition and exhibited as fold change.

*MTT assay:* Primary hippocampal cultures were incubated for 24 or 48 hours in the presence of palmitate (50-500 μM) or vehicle, and cell viability was assessed using the MTT (3-[4,5-dimethyl-thiazol-2-yl]-2,5- diphenyl tetrazolium bromide) reduction assay (Boehringer Mannheim, Indianapolis, IN). Briefly, hippocampal cultures were incubated with a 0.5 mg/ml

solution of MTT at 37 °C for 4 h to allow reduction to formazan blue by metabolically active cells. Cells were then lysed, and formazan crystals were solubilized by incubation in 0.01 N HCl containing 10% SDS for 24 h at room temperature. Optical density at 570 nm was measured in a ThermoMax Microplate reader.

*Mouse perfusion and brain slices:* Male swiss mice (2-4-month old) were anesthetized with xylazine (10 mg/kg) and ketamine (100 mg/kg), and they were perfused intracardiacally with PBS followed by 4% paraformaldehyde (PFA). Brains were dissected and post-fixed by immersion in 4% PFA for 24 hours. After washing with PBS, brains were placed sequentially in 20% and 30% sucrose solutions, they were embedded in Tissue-Tek O.C.T. compound (Sakura) and frozen in dry ice. Ten µm thickness coronal brain sections (from Bregma -1.34 mm to Bregma -2.06 mm) (Paxinos and Franklin, 2004) were cut in a cryostat (Leica CM1850) and placed on poly-l-lysine (200 µg/mL) coated slides. The slides were maintained at room temperature overnight for complete adhesion of the sections, and then they were frozen at -20 ºC until use.

*Immunohistochemistry and image analysis:* Hippocampal sections were equilibrated at RT, washed with PBS and blocked with 10% bovine serum albumin in 0.25%Triton X-100/PBS (PBS-T) for 1 hour at RT. Thereafter, sections were incubated with primary antibody (anti-Iba-1, Wako, 1:500 diluition or anti-GFAP, Dako, 1:1,000 diluition) diluited in PBS-T overnight at RT. Sections were rinsed with PBS, and incubated with Alexa Fluor 488-conjugated anti-rabbit IgG secondary antibody (1:2,000 diluition, Molecular Probes) diluited in PBS-T for 2h at RT. Then, sections were rinsed with PBS and mounted with Prolong Gold mouting medium with DAPI (Molecular Probes). The dentate gyrus (DG) of hippocampus was analyzed as follows. Two to four coronal brain sections (50 µm apart from each other) were sampled per animal, and a part of the DG from both hemispheres were imaged whenever it was possible. Images (12 bit) were acquired with AxioCam MR R3 camera and Zeiss Axio Imager M2 microscope or AxioCam MRm and Zeiss Axio Observer Z1 microscope using 20× objective under conventional fluorescence microscopy. Primary antibody was omitted

from negative control sections, and secondary antibody did not show unspecific immunolabeling.

A region of interest (ROI) was delimited in the DG, its area was measured using ImageJ software (NIH) and the number of Iba-1-positive cells was counted. The graphs represent the number of Iba-1-positive cells per $mm^2$. Similarly, for GFAP analysis, a ROI was delimited in the DG and the intensity of GFAP immunoreactivity was measured in 8-bit grayscale photomicrographies, such that Raw Integrated Density per $\mu m^2$ was represented in the graphs.

## QUANTIFICATION AND STATISTICAL ANALYSIS

Human data was analyzed in 49 subjects classified as normal weight, overweight or obese according BMI (Table S1). Correlation was calculated using linear regression (r2 and p values as indicated in "Figure Legends"). In results were data was presented as mean ± SEM (see "Figure Legends"), statistical significance was determined using one-way ANOVA followed by Holm-Sidak`s *post hoc* test.

Experiments using mice models were performed with groups of 5 to 12 mice per experimental condition, as indicated in "Figure Legends". Data are presented as means ± SEM and outliers are detected and removed from analysis using Grubbs ($\alpha = 0.05$) or ROUT ($Q = 1\%$) tests. Statistical significance was determined using two-tailed t-test (paired or unpaired) and one-way or two-way ANOVA, with suitable *post hoc* analysis (see in "Figure Legends").

Experiments using cell culture were performed in 3 - 4 independent cultures. Data are presented as means ± SEM and statistical significance was determined using two-tailed t-test (paired or unpaired) and one-way or two-way ANOVA, with suitable *post hoc* analysis (see in "Figure Legends").

In general, experimental data were plotted using GraphPad Prism software. Details of statistical analysis and number of biological replicates are indicated in the respective figure legend.

## DATA AND CODE AVAILABILITY

This study did not generate/analyze datasets or code.

## References


Ajuwon, K.M., and Spurlock, M.E. (2005). Palmitate Activates the NF-κB Transcription Factor and Induces IL-6 and TNFα Expression in 3T3-L1 Adipocytes. J. Nutr. *135*, 1841–1846.

Albert, M.S., DeKosky, S.T., Dickson, D., Dubois, B., Feldman, H.H., Fox, N.C., Gamst, A., Holtzman, D.M., Jagust, W.J., Petersen, R.C., et al. (2011). The diagnosis of mild cognitive impairment due to Alzheimer's disease: Recommendations from the National Institute on Aging-Alzheimer's Association workgroups on diagnostic guidelines for Alzheimer's disease. Alzheimer's Dement. *7*, 270–279.

Arnold, S.E., Lucki, I., Brookshire, B.R., Carlson, G.C., Browne, C.A., Kazi, H., Bang, S., Choi, B.-R., Chen, Y., McMullen, M.F., et al. (2014). High fat diet produces brain insulin resistance, synaptodendritic abnormalities and altered behavior in mice. Neurobiol. Dis. *67*, 79–87.

Arruda, A.P., Milanski, M., Coope, A., Torsoni, A.S., Ropelle, E., Carvalho, D.P., Carvalheira, J.B., and Velloso, L.A. (2011). Low-Grade Hypothalamic Inflammation Leads to Defective Thermogenesis, Insulin Resistance, and Impaired Insulin Secretion. Endocrinology *152*, 1314–1326.

Azevedo, E.P., Ledo, J.H., Barbosa, G., Sobrinho, M., Diniz, L., Fonseca, A.C.C., Gomes, F., Romão, L., Lima, F.R.S., Palhano, F.L., et al. (2013). Activated microglia mediate synapse loss and short-term memory deficits in a mouse model of tran. Cell Death Dis. *4*.

Benoit, S.C., Kemp, C.J., Elias, C.F., Abplanalp, W., Herman, J.P., Migrenne, S., Lefevre, A.-L., Cruciani-Guglielmacci, C., Magnan, C., Yu, F., et al. (2009). Palmitic acid mediates hypothalamic insulin resistance by altering PKC-theta subcellular localization in rodents. J. Clin. Invest. *119*, 2577–2589.

Brewer, G.J. (1997). Isolation and culture of adult rat hippocampal neurons. J. Neurosci. Methods *71*, 143–155.

Chan, J.M., Rimm, E.B., Colditz, G.A., Stampfer, M.J., and Willett, W.C. (1994). Obesity, fat distribution, and weight gain as risk factors for clinical diabetes in men. Diabetes Care *17*, 961–969.

Cheng, L., Yu, Y., Szabo, A., Wu, Y., Wang, H., Camer, D., and Huang, X.-F. (2015). Palmitic acid induces central leptin resistance and impairs hepatic glucose and lipid metabolism in male mice. J. Nutr. Biochem. *26*, 541–548.

Chiu, S.-L., Chen, C.-M., and Cline, H.T. (2008). Insulin receptor signaling regulates synapse number, dendritic plasticity, and circuit function in vivo. Neuron *58*, 708–719.

Clarke, J.R., Lyra E Silva, N.M., Figueiredo, C.P., Frozza, R.L., Ledo, J.H., Beckman, D., Katashima, C.K., Razolli, D., Carvalho, B.M., Frazão, R., et al. (2015). Alzheimer-associated Aβ oligomers impact the central nervous system to induce peripheral metabolic deregulation. EMBO Mol. Med. *7*, 190–210.

Elias, M.F., Elias, P.K., Sullivan, L.M., Wolf, P.A., and D'Agostino, R.B. (2003). Lower cognitive function in the presence of obesity and hypertension: the Framingham heart study. Int. J. Obes. Relat. Metab. Disord. *27*, 260–268.

De Felice, F.G., Vieira, M.N.N., Bomfim, T.R., Decker, H., Velasco, P.T., Lambert, M.P., Viola, K.L., Zhao, W.-Q., Ferreira, S.T., and Klein, W.L. (2009). Protection of synapses against Alzheimer's-linked toxins: insulin signaling prevents the pathogenic binding of Abeta oligomers. Proc. Natl. Acad. Sci. U. S. A. *106*, 1971–1976.

Fernández-Real, J.-M., Broch, M., Vendrell, J., and Ricart, W. (2003). Insulin resistance, inflammation, and serum fatty acid composition. Diabetes Care *26*, 1362–1368.

Figueiredo, C.P., Clarke, J.R., Ledo, J.H., Ribeiro, F.C., Costa, C. V., Melo, H.M., Mota-Sales, A.P., Saraiva, L.M., Klein, W.L., Sebollela, A., et al. (2013). Memantine rescues transient cognitive impairment caused by high-molecular-weight Aβ oligomers but not the persistent impairment induced by low-molecular-weight oligomers. J. Neurosci. *33*, 9626–9634.

Franklin, K.B.J., and Paxinos, G. Paxinos and Franklin's The mouse brain in stereotaxic coordinates.

Garvey, W.T., Mechanick, J.I., Brett, E.M., Garber, A.J., Hurley, D.L., Jastreboff, A.M., Nadolsky, K., Pessah-Pollack, R., and Plodkowski, R. (2016). American association of clinical endocrinologists and American college of endocrinology comprehensive clinical practice guidelines for medical care of patients with obesity. Endocr. Pract. *22*, 1–203.

Ginneken, V. van, Verheij, E., Hekman, M., and der Greef, J. van (2017). Characterization of the lipid profile post mortem for Type-2 diabetes in human brain and plasma of the elderly with LCMS-techniques: a descriptive approach of diabetic encephalopathy. Integr. Mol. Med. *4*.

Gregor, M.F., and Hotamisligil, G.S. (2011). Inflammatory mechanisms in obesity. Annu. Rev. Immunol. *29*, 415–445.

Gruart, A., Muñoz, M.D., and Delgado-Garcia, J.M. (2006). Involvement of the CA3–CA1 synapse in the acquisition of associative learning in behaving mice. J. Neurosci. *26*, 1077–1087.

Guh, D.P., Zhang, W., Bansback, N., Amarsi, Z., Birmingham, C.L., and Anis, A.H. (2009). The incidence of co-morbidities related to obesity and overweight: a systematic review and

meta-analysis. BMC Public Health *9*, 88.

Gustafson, D. (2006). Adiposity indices and dementia. Lancet. Neurol. *5*, 713–720.

Gustafson, D., Lissner, L., Bengtsson, C., Björkelund, C., and Skoog, I. (2004). A 24-year follow-up of body mass index and cerebral atrophy. Neurology *63*, 1876–1881.

Hanisch, U.K., and Kettenmann, H. (2007). Microglia: Active sensor and versatile effector cells in the normal and pathologic brain. Nat. Neurosci. *10*, 1387–1394.

Heneka, M.T., Kummer, M.P., and Latz, E. (2014). Innate immune activation in neurodegenerative disease. Nat. Rev. Immunol. *14*, 463–477.

Ho, A.J., Raji, C.A., Becker, J.T., Lopez, O.L., Kuller, L.H., Hua, X., Lee, S., Hibar, D., Dinov, I.D., Stein, J.L., et al. (2010). Obesity is linked with lower brain volume in 700 AD and MCI patients. Neurobiol. Aging *31*, 1326–1339.

Holland, W.L., Bikman, B.T., Wang, L.-P., Yuguang, G., Sargent, K.M., Bulchand, S., Knotts, T.A., Shui, G., Clegg, D.J., Wenk, M.R., et al. (2011). Lipid-induced insulin resistance mediated by the proinflammatory receptor TLR4 requires saturated fatty acid-induced ceramide biosynthesis in mice. J. Clin. Invest. *121*, 1858–1870.

Hotamisligil, G.S. (1999). The role of TNFalpha and TNF receptors in obesity and insulin resistance. J. Intern. Med. *245*, 621–625.

Hotamisligil, G.S. (2017). Inflammation, metaflammation and immunometabolic disorders. Nature *542*, 177–185.

Hotamisligil, G.S., and Spiegelman, B.M. (1994). Tumor Necrosis Factor : A Key Component of the Obesity-Diabetes Link. Diabetes *43*, 1271–1278.

Hotamisligil, G.S., Shargill, N.S., and Spiegelman, B.M. (1993). Adipose expression of tumor necrosis factor-alpha: direct role in obesity-linked insulin resistance. Science *259*, 87–91.

Hotamisligil, G.S., Arner, P., Caro, J.F., Atkinson, R.L., and Spiegelman, B.M. (1995). Increased adipose tissue expression of tumor necrosis factor-alpha in human obesity and insulin resistance. J. Clin. Invest. *95*, 2409–2415.

Hotamisligil, G.S., Peraldi, P., Budavari, A., Ellis, R., White, M.F., and Spiegelman, B.M. (1996). IRS-1-mediated inhibition of insulin receptor tyrosine kinase activity in TNF-alpha- and obesity-induced insulin resistance. Science *271*, 665–668.

Hu, F.B., Manson, J.E., Stampfer, M.J., Colditz, G., Liu, S., Solomon, C.G., and Willett, W.C. (2001). Diet, lifestyle, and the risk of type 2 diabetes mellitus in women. N. Engl. J. Med. *345*, 790–797.

Janssen, I., Katzmarzyk, P.T., and Ross, R. (2002). Body mass index, waist circumference,

and health risk: evidence in support of current National Institutes of Health guidelines. Arch. Intern. Med. *162*, 2074–2079.

Jeon, B.T., Jeong, E.A., Shin, H.J., Lee, Y., Lee, D.H., Kim, H.J., Kang, S.S., Cho, G.J., Choi, W.S., and Roh, G.S. (2012). Resveratrol attenuates obesity-associated peripheral and central inflammation and improves memory deficit in mice fed a high-fat diet. Diabetes *61*, 1444–1454.

Jové, M., Planavila, A., Sánchez, R.M., Merlos, M., Laguna, J.C., and Vázquez-Carrera, M. (2006). Palmitate induces tumor necrosis factor-alpha expression in C2C12 skeletal muscle cells by a mechanism involving protein kinase C and nuclear factor-kappaB activation. Endocrinology *147*, 552–561.

Kalmijn, S., Van Boxtel, M.P.J., Ocké, M., Verschuren, W.M.M., Kromhout, D., and Launer, L.J. (2004). Dietary intake of fatty acids and fish in relation to cognitive performance at middle age. Neurology *62*, 275–280.

Karmi, A., Iozzo, P., Viljanen, A., Hirvonen, J., Fielding, B.A., Virtanen, K., Oikonen, V., Kemppainen, J., Viljanen, T., Guiducci, L., et al. (2010). Increased brain fatty acid uptake in metabolic syndrome. Diabetes *59*, 2171–2177.

Kivipelto, M., Ngandu, T., Fratiglioni, L., Viitanen, M., Kåreholt, I., Winblad, B., Helkala, E.-L., Tuomilehto, J., Soininen, H., and Nissinen, A. (2005). Obesity and vascular risk factors at midlife and the risk of dementia and Alzheimer disease. Arch. Neurol. *62*, 1556–1560.

Knight, E.M., Martins, I.V.A., Gümüsgöz, S., Allan, S.M., and Lawrence, C.B. (2014). High-fat diet-induced memory impairment in triple-transgenic Alzheimer's disease (3xTgAD) mice is independent of changes in amyloid and tau pathology. Neurobiol. Aging *35*, 1821–1832.

Laursen SE, B.J. (1986). Intracerebroventricular injections in mice. Some methodological refinements. J Pharmacol Methods. *16*, 355–357.

Ledo, J.H., Azevedo, E.P., Clarke, J.R., Ribeiro, F.C., Figueiredo, C.P., Foguel, D., De Felice, F.G., and Ferreira, S.T. (2013). Amyloid-β oligomers link depressive-like behavior and cognitive deficits in mice. Mol. Psychiatry *18*, 1053–1054.

Ledo, J.H., Azevedo, E.P., Beckman, D., Ribeiro, F.C., Santos, L.E., Razolli, D.S., Kincheski, G.C., Melo, H.M., Bellio, M., Teixeira, A.L., et al. (2016). Cross Talk Between Brain Innate Immunity and Serotonin Signaling Underlies Depressive-Like Behavior Induced by Alzheimer's Amyloid-β Oligomers in Mice. J. Neurosci. *36*, 12106–12116.

Lee, C.-C., Huang, C.-C., and Hsu, K.-S. (2011). Insulin promotes dendritic spine and synapse formation by the PI3K/Akt/mTOR and Rac1 signaling pathways. Neuropharmacology *61*, 867–879.

Liu, L., Martin, R., and Chan, C. (2013). Palmitate-activated astrocytes via serine palmitoyltransferase increase BACE1 in primary neurons by sphingomyelinases. Neurobiol.

Aging *34*, 540–550.

Lourenco, M. V, Clarke, J.R., Frozza, R.L., Bomfim, T.R., Forny-Germano, L., Batista, A.F., Sathler, L.B., Brito-Moreira, J., Amaral, O.B., Silva, C.A., et al. (2013). TNF-α mediates PKR-dependent memory impairment and brain IRS-1 inhibition induced by Alzheimer's β-amyloid oligomers in mice and monkeys. Cell Metab. *18*, 831–843.

Madronal, N., Delgado-Garcia, J.M., and Gruart, A. (2007). Differential Effects of Long-Term Potentiation Evoked at the CA3 CA1 Synapse before, during, and after the Acquisition of Classical Eyeblink Conditioning in Behaving Mice. J. Neurosci. *27*, 12139–12146.

Magalhães, T.N.C., Weiler, M., Teixeira, C.V.L., Hayata, T., Moraes, A.S., Boldrini, V.O., Dos Santos, L.M., de Campos, B.M., de Rezende, T.J.R., Joaquim, H.P.G., et al. (2018). Systemic Inflammation and Multimodal Biomarkers in Amnestic Mild Cognitive Impairment and Alzheimer's Disease. Mol. Neurobiol. *55*, 5689–5697.

Marwarha, G., Claycombe, K., Schommer, J., Collins, D., and Ghribi, O. (2016). Palmitate-induced Endoplasmic Reticulum stress and subsequent C/EBPα Homologous Protein activation attenuates leptin and Insulin-like growth factor 1 expression in the brain. Cell. Signal. *28*, 1789–1805.

Mayer, C.M., and Belsham, D.D. (2010). Palmitate attenuates insulin signaling and induces endoplasmic reticulum stress and apoptosis in hypothalamic neurons: rescue of resistance and apoptosis through adenosine 5' monophosphate-activated protein kinase activation. Endocrinology *151*, 576–585.

Mayer, E.J., Newman, B., Quesenberry, C.P., and Selby, J. V (1993). Usual dietary fat intake and insulin concentrations in healthy women twins. Diabetes Care *16*, 1459–1469.

McCoy, M.K., and Tansey, M.G. (2008). TNF signaling inhibition in the CNS: Implications for normal brain function and neurodegenerative disease. J. Neuroinflammation *5*.

Meek, S.E., Nair, K.S., and Jensen, M.D. (1999). Insulin regulation of regional free fatty acid metabolism. Diabetes *48*, 10–14.

Milanski, M., Degasperi, G., Coope, A., Morari, J., Denis, R., Cintra, D.E., Tsukumo, D.M.L., Anhe, G., Amaral, M.E., Takahashi, H.K., et al. (2009). Saturated fatty acids produce an inflammatory response predominantly through the activation of TLR4 signaling in hypothalamus: implications for the pathogenesis of obesity. J. Neurosci. *29*, 359–370.

Mokdad, A.H., Ford, E.S., Bowman, B.A., Dietz, W.H., Vinicor, F., Bales, V.S., and Marks, J.S. (2003). Prevalence of obesity, diabetes, and obesity-related health risk factors, 2001. J. Am. Med. Assoc. *289*, 76–79.

Morris, M.C., Evans, D.A., Bienias, J.L., Tangney, C.C., Bennett, D.A., Aggarwal, N., Schneider, J., and Wilson, R.S. (2003). Dietary fats and the risk of incident Alzheimer disease. Arch. Neurol. *60*, 194–200.

Must, A., Spadano, J., Coakley, E.H., Field, A.E., Colditz, G., and Dietz, W.H. (1999). The disease burden associated with overweight and obesity. JAMA *282*, 1523–1529.

Nakamura, S., Takamura, T., Matsuzawa-Nagata, N., Takayama, H., Misu, H., Noda, H., Nabemoto, S., Kurita, S., Ota, T., Ando, H., et al. (2009). Palmitate induces insulin resistance in H4IIEC3 hepatocytes through reactive oxygen species produced by mitochondria. J. Biol. Chem. *284*, 14809–14818.

Ott, A., Stolk, R.P., Hofman, A., van Harskamp, F., Grobbee, D.E., and Breteler, M.M. (1996). Association of diabetes mellitus and dementia: the Rotterdam Study. Diabetologia *39*, 1392–1397.

Parker, D.R., Weiss, S.T., Troisi, R., Cassano, P.A., Vokonas, P.S., and Landsberg, L. (1993). Relationship of dietary saturated fatty acids and body habitus to serum insulin concentrations: the Normative Aging Study. Am. J. Clin. Nutr. *58*, 129–136.

Pfeffer, K., Matsuyama, T., Kündig, T.M., Wakeham, A., Kishihara, K., Shahinian, A., Wiegmann, K., Ohashi, P.S., Krönke, M., and Mak, T.W. (1993). Mice deficient for the 55 kd tumor necrosis factor receptor are resistant to endotoxic shock, yet succumb to L. monocytogenes infection. Cell *73*, 457–467.

Pilitsis, J.G., Diaz, F.G., Wellwood, J.M., Oregan, M.H., Fairfax, M.R., Phillis, J.W., and Coplin, W.M. (2001). Quantification of free fatty acids in human cerebrospinal fluid. Neurochem. Res. *26*, 1265–1270.

Quehenberger, O., Armando, A.M., Brown, A.H., Milne, S.B., Myers, D.S., Merrill, A.H., Bandyopadhyay, S., Jones, K.N., Kelly, S., Shaner, R.L., et al. (2010). Lipidomics reveals a remarkable diversity of lipids in human plasma1. J. Lipid Res. *51*, 3299–3305.

Rabelo, A.G., Teixeira, C.V., Magalhães, T.N., Carletti-Cassani, A.F.M., Amato Filho, A.C., Joaquim, H.P., Talib, L.L., Forlenza, O., Ribeiro, P.A., Secolin, R., et al. (2017). Is cerebral microbleed prevalence relevant as a biomarker in amnestic mild cognitive impairment and mild Alzheimer's disease? Neuroradiol. J. *30*, 477–485.

Raj, A., Kuceyeski, A., and Weiner, M. (2012). A network diffusion model of disease progression in dementia. Neuron *73*, 1204–1215.

Razolli, D.S., Moraes, J.C., Morari, J., Moura, R.F., Vinolo, M.A., and Velloso, L.A. (2015). TLR4 Expression in Bone Marrow-Derived Cells Is Both Necessary and Sufficient to Produce the Insulin Resistance Phenotype in Diet-Induced Obesity.

Roberts, R.O., Knopman, D.S., Przybelski, S.A., Mielke, M.M., Kantarci, K., Preboske, G.M., Senjem, M.L., Pankratz, V.S., Geda, Y.E., Boeve, B.F., et al. (2014). Association of type 2 diabetes with brain atrophy and cognitive impairment. Neurology *82*, 1132–1141.

Roust, L.R., and Jensen, M.D. (1993). Postprandial free fatty acid kinetics are abnormal in upper body obesity. Diabetes *42*, 1567–1573.

Schindelin, J., Arganda-Carreras, I., Frise, E., Kaynig, V., Longair, M., Pietzsch, T., Preibisch, S., Rueden, C., Saalfeld, S., Schmid, B., et al. (2012). Fiji: An open-source platform for biological-image analysis. Nat. Methods *9*, 676–682.

Shi, H., Yin, H., Flier, J.S., Shi, H., Kokoeva, M. V, Inouye, K., Tzameli, I., Yin, H., and Flier, J.S. (2006). TLR4 links innate immunity and fatty acid – induced insulin resistance Find the latest version : TLR4 links innate immunity and fatty acid – induced insulin resistance. J. Clin. Invest. *116*, 3015–3025.

Shirai, N., Suzuki, H., and Wada, S. (2005). Direct methylation from mouse plasma and from liver and brain homogenates. Anal. Biochem. *343*, 48–53.

Spiegelman, B.M., and Flier, J.S. (2001). Obesity and the regulation of energy balance. Cell *104*, 531–543.

Spinelli, M., Fusco, S., Mainardi, M., Scala, F., Natale, F., Lapenta, R., Mattera, A., Rinaudo, M., Donatella, D., Puma, L., et al. (2017). Brain insulin resistance impairs hippocampal synaptic plasticity and memory by increasing GluA1 palmitoylation through FoxO3a. Nat. Commun. *8*, 1–14.

Sunyer, B., Patil, S., and Lubec, G. (2014). Barnes maze , a useful task to assess spatial reference memory in the mice. 1–13.

Takechi, R., Lam, V., Brook, E., Giles, C., Fimognari, N., Mooranian, A., Al-Salami, H., Coulson, S.H., Nesbit, M., and Mamo, J.C.L. (2017). Blood-Brain Barrier Dysfunction Precedes Cognitive Decline and Neurodegeneration in Diabetic Insulin Resistant Mouse Model: An Implication for Causal Link. Front. Aging Neurosci. *9*, 399.

Takeda, S., Sato, N., Uchio-Yamada, K., Sawada, K., Kunieda, T., Takeuchi, D., Kurinami, H., Shinohara, M., Rakugi, H., and Morishita, R. (2010). Diabetes-accelerated memory dysfunction via cerebrovascular inflammation and Abeta deposition in an Alzheimer mouse model with diabetes. Proc. Natl. Acad. Sci. U. S. A. *107*, 7036–7041.

Teixeira, C.V.L., Rezende, T.J.R., Weiler, M., Nogueira, M.H., Campos, B.M., Pegoraro, L.F.L., Vicentini, J.E., Scriptore, G., Cendes, F., and Balthazar, M.L.F. (2016). Relation between aerobic fitness and brain structures in amnestic mild cognitive impairment elderly. Age (Dordr). *38*, 51.

Teixeira, C.V.L., Ribeiro de Rezende, T.J., Weiler, M., Magalhães, T.N.C., Carletti-Cassani, A.F.M.K., Silva, T.Q.A.C., Joaquim, H.P.G., Talib, L.L., Forlenza, O.V., Franco, M.P., et al. (2018). Cognitive and structural cerebral changes in amnestic mild cognitive impairment due to Alzheimer's disease after multicomponent training. Alzheimer's Dement. (New York, N. Y.) *4*, 473–480.

Thaler, J.P., Yi, C.X., Schur, E.A., Guyenet, S.J., Hwang, B.H., Dietrich, M.O., Zhao, X., Sarruf, D.A., Izgur, V., Maravilla, K.R., et al. (2012). Obesity is associated with hypothalamic injury in rodents and humans. J. Clin. Invest. *122*, 153–162.

Valdearcos, M., Robblee, M.M., Benjamin, D.I., Nomura, D.K., Xu, A.W., and Koliwad, S.K. (2014). Microglia Dictate the Impact of Saturated Fat Consumption on Hypothalamic Inflammation and Neuronal Function. Cell Rep. *9*, 2124–2138.

Vessby, B., Uusitupa, M., Hermansen, K., Riccardi, G., Rivellese, A.A., Tapsell, L.C., Nälsén, C., Berglund, L., Louheranta, A., Rasmussen, B.M., et al. (2001). Substituting dietary saturated for monounsaturated fat impairs insulin sensitivity in healthy men and women: The KANWU Study. Diabetologia *44*, 312–319.

Weiler, M., Machado de Campos, B., Vieira de Ligo Teixeira, C., Casseb, R.F., Mac Knight Carletti-Cassani, A.F., Vicentini, J.E., Cardoso Magalhães, T.N., Talib, L.L., Forlenza, O.V., and Figueredo Balthazar, M.L. (2017). Intranetwork and internetwork connectivity in patients with Alzheimer disease and the association with cerebrospinal fluid biomarker levels. J. Psychiatry Neurosci. *42*, 366–377.

Whitmer, R.A., Gustafson, D.R., Barrett-Connor, E., Haan, M.N., Gunderson, E.P., and Yaffe, K. (2008). Central obesity and increased risk of dementia more than three decades later. Neurology *71*, 1057–1064.

Wilson, P.W.F., D'Agostino, R.B., Sullivan, L., Parise, H., and Kannel, W.B. (2002). Overweight and obesity as determinants of cardiovascular risk: the Framingham experience. Arch. Intern. Med. *162*, 1867–1872.

Wyss-Coray, T., and Mucke, L. (2002). Inflammation in neurodegenerative disease--a double-edged sword. Neuron *35*, 419–432.

Yuzefovych, L., Wilson, G., and Rachek, L. (2010). Different effects of oleate vs. palmitate on mitochondrial function, apoptosis, and insulin signaling in L6 skeletal muscle cells: role of oxidative stress. Am. J. Physiol. Endocrinol. Metab. *299*, E1096-105.

Zhao, W., Wu, X., Xie, H., Ke, Y., and Yung, W.-H. (2010). Permissive role of insulin in the expression of long-term potentiation in the hippocampus of immature rats. Neurosignals. *18*, 236–245.

**Keywords:** palmitate, memory impairment, obesity, brain inflammation, microglia, TNF-α.

**Highlights and eTOC Blurb**

**Highlights:**

- Palmitate is increased in the CSF of overweight and obese humans with aMCI.
- CSF palmitate inversely correlates with cognitive performance in overweight humans.
- Palmitate impairs synaptic plasticity and memory in mice.
- Activated microglia and TNF-α mediate palmitate-induced impairments in memory.

**eTOC Blurb:**

Obesity has been associated with cognitive decline. Melo et al. show that palmitate levels are increased in the CSF of overweight and obese humans. In mice, intracerebroventricular infusion of palmitate impaired synaptic plasticity and memory. Microglial-derived TNF-α was found to mediate the deleterious actions of palmitate in the brain.

## KEY RESOURCES TABLE

The table highlights the genetically modified organisms and strains, cell lines, reagents, software, and source data **essential** to reproduce results presented in the manuscript. Depending on the nature of the study, this may include standard laboratory materials (i.e., food chow for metabolism studies), but the Table is **not** meant to be comprehensive list of all materials and resources used (e.g., essential chemicals such as SDS, sucrose, or standard culture media don't need to be listed in the Table). **Items in the Table must also be reported in the Method Details section within the context of their use.** The number of **primers and RNA sequences** that may be listed in the Table is restricted to no more than ten each. If there are more than ten primers or RNA sequences to report, please provide this information as a supplementary document and reference this file (e.g., See Table S1 for XX) in the Key Resources Table.

***Please note that ALL references cited in the Key Resources Table must be included in the References list.*** Please report the information as follows:

- **REAGENT or RESOURCE:** Provide full descriptive name of the item so that it can be identified and linked with its description in the manuscript (e.g., provide version number for software, host source for antibody, strain name). In the Experimental Models section, please include all models used in the paper and describe each line/strain as: model organism: name used for strain/line in paper: genotype. (i.e., Mouse: $OXTR^{fl/fl}$: B6.129(SJL)-$Oxtr^{tm1.1Wsy/J}$). In the Biological Samples section, please list all samples obtained from commercial sources or biological repositories. Please note that software mentioned in the Methods Details or Data and Software Availability section needs to be also included in the table. See the sample Table at the end of this document for examples of how to report reagents.

- **SOURCE:** Report the company, manufacturer, or individual that provided the item or where the item can obtained (e.g., stock center or repository). For materials distributed by Addgene, please cite the article describing the plasmid and include "Addgene" as part of the identifier. If an item is from another lab, please include the name of the principal investigator and a citation if it has been previously published. If the material is being reported for the first time in the current paper, please indicate as "this paper." For software, please provide the company name if it is commercially available or cite the paper in which it has been initially described.

- **IDENTIFIER:** Include catalog numbers (entered in the column as "Cat#" followed by the number, e.g., Cat#3879S). Where available, please include unique entities such as RRIDs, Model Organism Database numbers, accession numbers, and PDB or CAS IDs. For antibodies, if applicable and available, please also include the lot number or clone identity. For software or data resources, please include the URL where the resource can be downloaded. Please ensure accuracy of the identifiers, as they are essential for generation of hyperlinks to external sources when available. Please see the Elsevier list of Data Repositories with automated bidirectional linking for details. When listing more than one identifier for the same item, use semicolons to separate them (e.g. Cat#3879S; RRID: AB_2255011). If an identifier is not available, please enter "N/A" in the column.
    - ***A NOTE ABOUT RRIDs:*** We highly recommend using RRIDs as the identifier (in particular for antibodies and organisms, but also for software tools and databases). For more details on how to obtain or generate an RRID for existing or newly generated resources, please visit the RII or search for RRIDs.

Please use the empty table that follows to organize the information in the sections defined by the subheading, skipping sections not relevant to your study. Please do not add subheadings. To add a row, place the cursor at the end of the row above where you would like to add the row, just outside the right border of the table. Then press the ENTER key to add the row. Please delete empty rows. Each entry must be on a separate row; do not list multiple items in a single table cell. Please see the sample table at the end of this document for examples of how reagents should be cited.

***TABLE FOR AUTHOR TO COMPLETE***

*Please upload the completed table as a separate document.* ***Please do not add subheadings to the Key Resources Table.*** *If you wish to make an entry that does not fall into one of the subheadings below, please contact your handling editor. (**NOTE:** For authors publishing in Current Biology, please note that references within the KRT should be in numbered style, rather than Harvard.)*

**KEY RESOURCES TABLE**

| REAGENT or RESOURCE | SOURCE | IDENTIFIER |
|---|---|---|
| **Antibodies** | | |
| Mouse monoclonal anti-Synaptophysin antibody | Abcam | Cat# ab8049; RRID: AB_2198854 |
| Rabbit polyclonal anti-Cyclophilin B antibody | Abcam | Cat# ab16045; RRID: AB_443295 |
| Rabbit polyclonal anti-PSD-95 antibody | Santa Cruz | Cat# SC 28941; RRID: AB_2092354 |
| Mouse monoclonal anti-beta Actin antibody | Abcam | Cat# ab6276; RRID: AB_2223210 |
| Rabbit polyclonal anti - pIRS-1 (Ser 612) antibody | Sigma - Aldrich | Cat# I2658 RRID: AB_260161 |
| Rabbit polyclonal anti - pIRS-1 (Ser 636) Antibody | Santa Cruz | Cat# SC 33957; RRID:AB_2125767 |
| Rabbit polyclonal anti - pIRS-1 (Ser307) antibody | Invitrogen | Cat# 44813G; RRID:AB_2533766 |
| Rabbit polyclonal anti - pIRS-1 (Ser312) antibody | Invitrogen | Cat# 44814G; RRID:AB_2533767 |
| Rabbit polyclonal anti Iba - 1 antibody | Wako | Cat# 019-19741; RRID:AB_839504 |
| Rabbit polyclonal anti - GFAP antibody | Wako | Cat# Z0334 RRID: AB_10013382 |
| Goat anti-Rabbit IgG (H+L) Cross-Adsorbed Secondary Antibody, Alexa Fluor 555 | Thermo Fisher Scientific | Cat# A-21428, RRID:AB_2535849 |
| Donkey anti-Rabbit IgG (H+L) Highly Cross-Adsorbed Secondary Antibody, Alexa Fluor 594, | Thermo Fisher Scientific | Cat# A-21207; RRID:AB_141637 |
| Goat anti-Mouse IgG (H+L) Cross-Adsorbed Secondary Antibody, Alexa Fluor 488 | Thermo Fisher Scientific | Cat# A-11001, RRID:AB_2534069 |
| Goat anti-Rabbit IgG (H+L) Cross-Adsorbed Secondary Antibody, Alexa Fluor 488 | Thermo Fisher Scientific | Cat# A-11008, RRID:AB_143165 |
| IRDye 800CW Goat anti-Mouse IgG (H + L) | Li-Cor Biosciences | Cat# 926-32210, RRID:AB_621842 |
| IRDye 680LT Goat anti-Rabbit IgG (H + L) | Li-Cor Biosciences | Cat# 926-68021, RRID: AB_10706309 |
| IRDye® 680LT Goat anti-Mouse IgG (H + L) | Li-Cor Biosciences | Cat# 925-68020, RRID: AB_2687826 |
| IRDye® 800CW Goat anti-Rabbit IgG (H + L) | Li-Cor Biosciences | Cat# 925-32211, RRID:AB_2651127 |
| **Chemicals, Peptides, and Recombinant Proteins** | | |
| Infliximab | Donated by Dr. Licio A. Velloso from the University of Campinas, São Paulo, Brazil. | N/A |

| | | |
|---|---|---|
| Minocycline hydrochloride | Sigma-Aldrich | Cat# M9511 |
| Sodium Palmitate | Sigma-Aldrich | Cat# P9767 |
| Sodium Oleate | Sigma-Aldrich | Cat# O7501 |
| Lipopolysaccharides from Escherichia coli | Sigma-Aldrich | Cat# L2880 |
| Thiazolyl Blue Tetrazolium Bromide | Sigma-Aldrich | Cat# M6494 |
| Bovine Serum Albumin | Sigma-Aldrich | Cat# A6003 |
| Tridecanoic acid (analytical standard) | Sigma Aldrich | Cat# 91988 |
| Boron trifluoride-methanol solution | Sigma Aldrich | Cat# 15716 |
| **Critical Commercial Assays** | | |
| Rat TNF-α ELISA MAX™ Deluxe | BioLegends | Cat# 438206 |
| Pierce BCA Protein Assay Kit | Invitrogen | Cat# 23225 |
| Super- Strand III Reverse Transcriptase kit | Invitrogen | Cat# 18080044 |
| High Capacity cDNA Reverse Transcription | Applied Biosystems | Cat# 4368814 |
| Power SYBR Green Master Mix | Thermo Fisher Scientific | Cat# 4367659 |
| **Deposited Data** | | |
| | | |
| **Experimental Models: Organisms/Strains** | | |
| Mouse: APPSwe/PS1DE9 mice | Jankowsky et al., 2001 - Federal University of Rio de Janeiro | N/A |
| Mouse:TNFRp55-/- (TNFR1 KO) mice | Arruda et al., 2011; Pfeffer et al., 1993 - Donated by Dr. Licio A. Velloso from the University of Campinas, São Paulo, Brazil | N/A |
| **Oligonucleotides** | | |
| rat ACTB *forward*: AGTGTGACGTTGACATCCGTA | This paper | N/A |
| rat ACTB *reverse*: GCCAGAGCAGTAATCTCCTTCT | This paper | N/A |
| rat INS 2 *forward*: CCTGCTCATCCTCTGGGAGC | This paper | N/A |
| rat INS 2 *reverse*: TGTGCACCTTGTGGGTCCTCCA | This paper | N/A |
| mice ACTB *forward*: GCCCTGAGGCTCTTTTCCAG | This paper | N/A |
| mice ACTB *reverse*: TGCCACAGGATTCCATACCC | This paper | N/A |
| mice TNF-α *forward*: CCCTCACACTCAGATCATCTTCT | Ledo et al., 2016 | N/A |
| mice TNF-α *reverse*: GCTACGACGTGGGCTACAG | Ledo et al., 2016 | N/A |
| Mice INS2 forward: ACATGGCCCTGTGGATGCGCT | This paper | N/A |
| Mice INS2 reverse: CACGGCGGGACATGGGTGTG | This paper | N/A |
| **Software and Algorithms** | | |
| GraphPad Prism software | This paper | https://www.graphpad.com/scientific-software/prism/ |
| Spike 2 | This paper | http://ced.co.uk/products/spkovin |

| | | |
|---|---|---|
| ANY-maze software | This paper | http://www.anymaze.co.uk/ |
| Fiji | Schindelin et al., 2012 | https://imagej.net/Fiji |
| **Other** | | |
| High fat diet | Razolli et al, 2015 - PragSoluções | N/A |
| | | |
| | | |
| | | |
| | | |

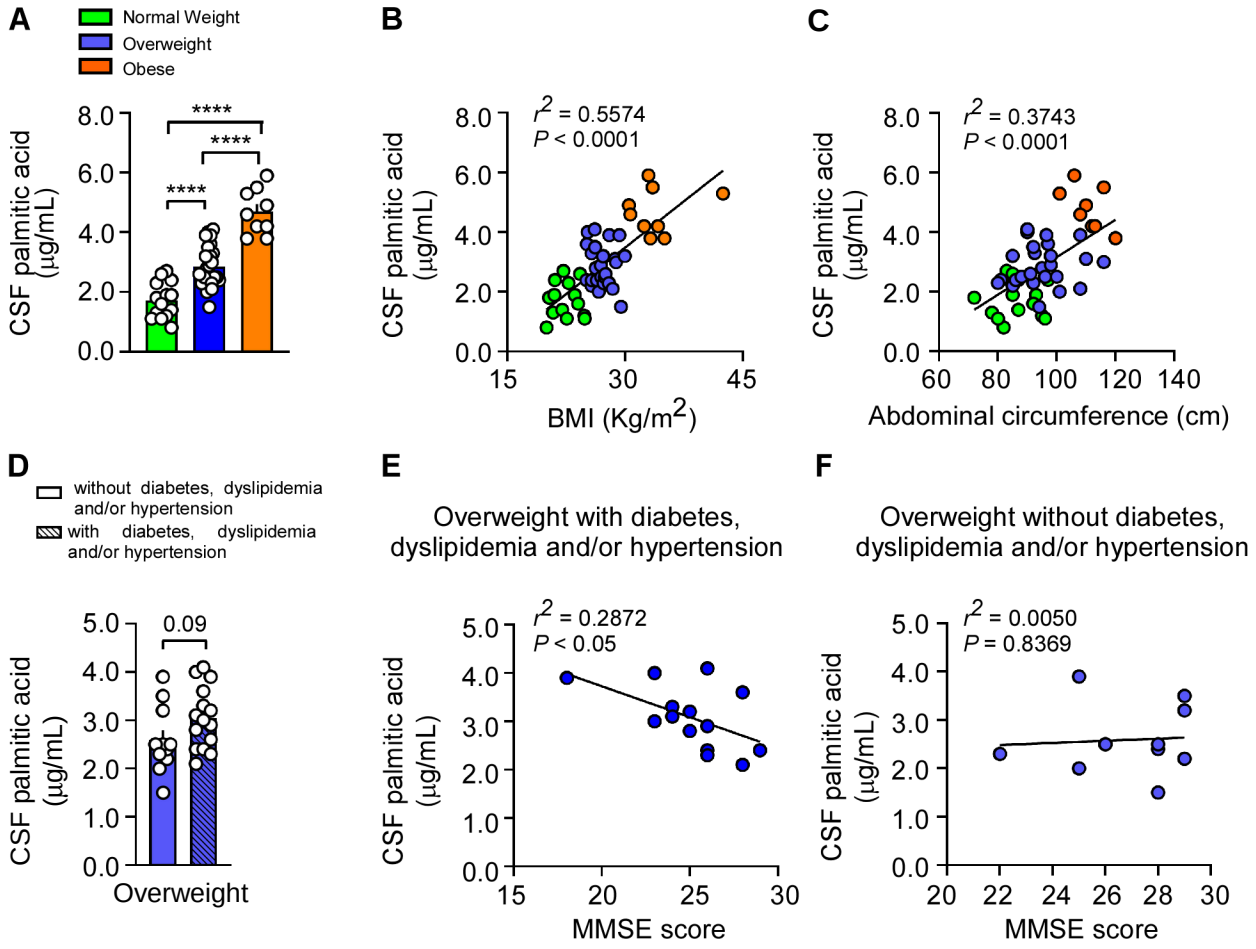
A
Normal Weight
Overweight
Obese
CSF palmitic acid (µg/mL)
****
****
****
B
$r^2$ = 0.5574
P < 0.0001
BMI (Kg/m$^2$)
C
$r^2$ = 0.3743
P < 0.0001
Abdominal circumference (cm)
D
without diabetes, dyslipidemia and/or hypertension
with diabetes, dyslipidemia and/or hypertension
0.09
Overweight
E
Overweight with diabetes, dyslipidemia and/or hypertension
$r^2$ = 0.2872
P < 0.05
MMSE score
F
Overweight without diabetes, dyslipidemia and/or hypertension
$r^2$ = 0.0050
P = 0.8369
MMSE score

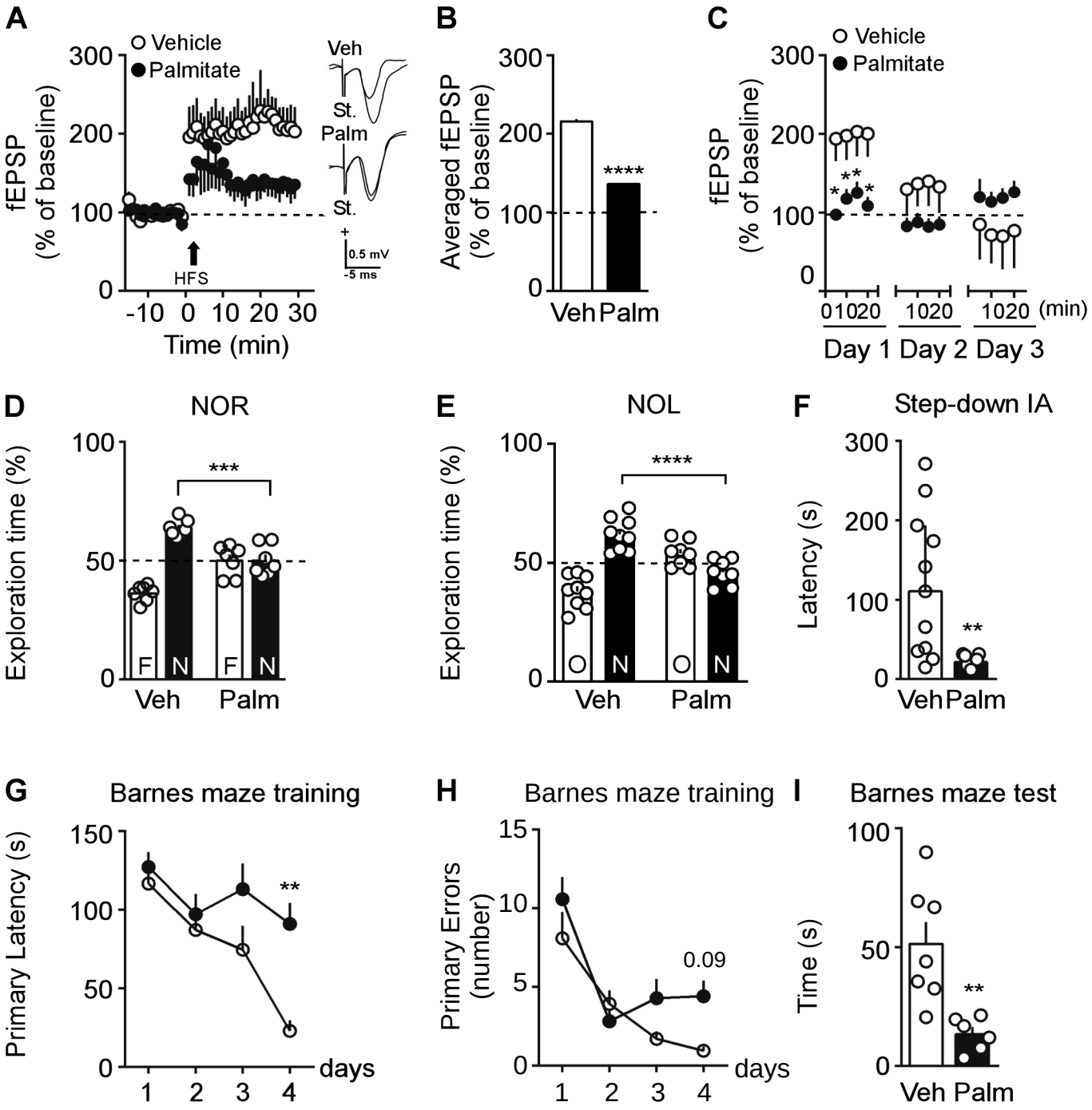
A
Vehicle
Palmitate
fEPSP (% of baseline)
300
200
100
0
Veh
St.
Palm
St.
+
0.5 mV
-5 ms
HFS
-10 0 10 20 30
Time (min)
B
Averaged fEPSP (% of baseline)
300
200
100
0
****
Veh Palm
C
Vehicle
Palmitate
fEPSP (% of baseline)
300
200
100
0
**
*
*
0 10 20 10 20 10 20 (min)
Day 1 Day 2 Day 3
D
NOR
Exploration time (%)
100
50
0
***
F N F N
Veh Palm
E
NOL
Exploration time (%)
100
50
0
****
O N O N
Veh Palm
F
Step-down IA
Latency (s)
300
200
100
0
**
Veh Palm
G
Barnes maze training
Primary Latency (s)
150
100
50
0
**
1 2 3 4
days
H
Barnes maze training
Primary Errors (number)
15
10
5
0
0.09
1 2 3 4
days
I
Barnes maze test
Time (s)
100
50
0
**
Veh Palm

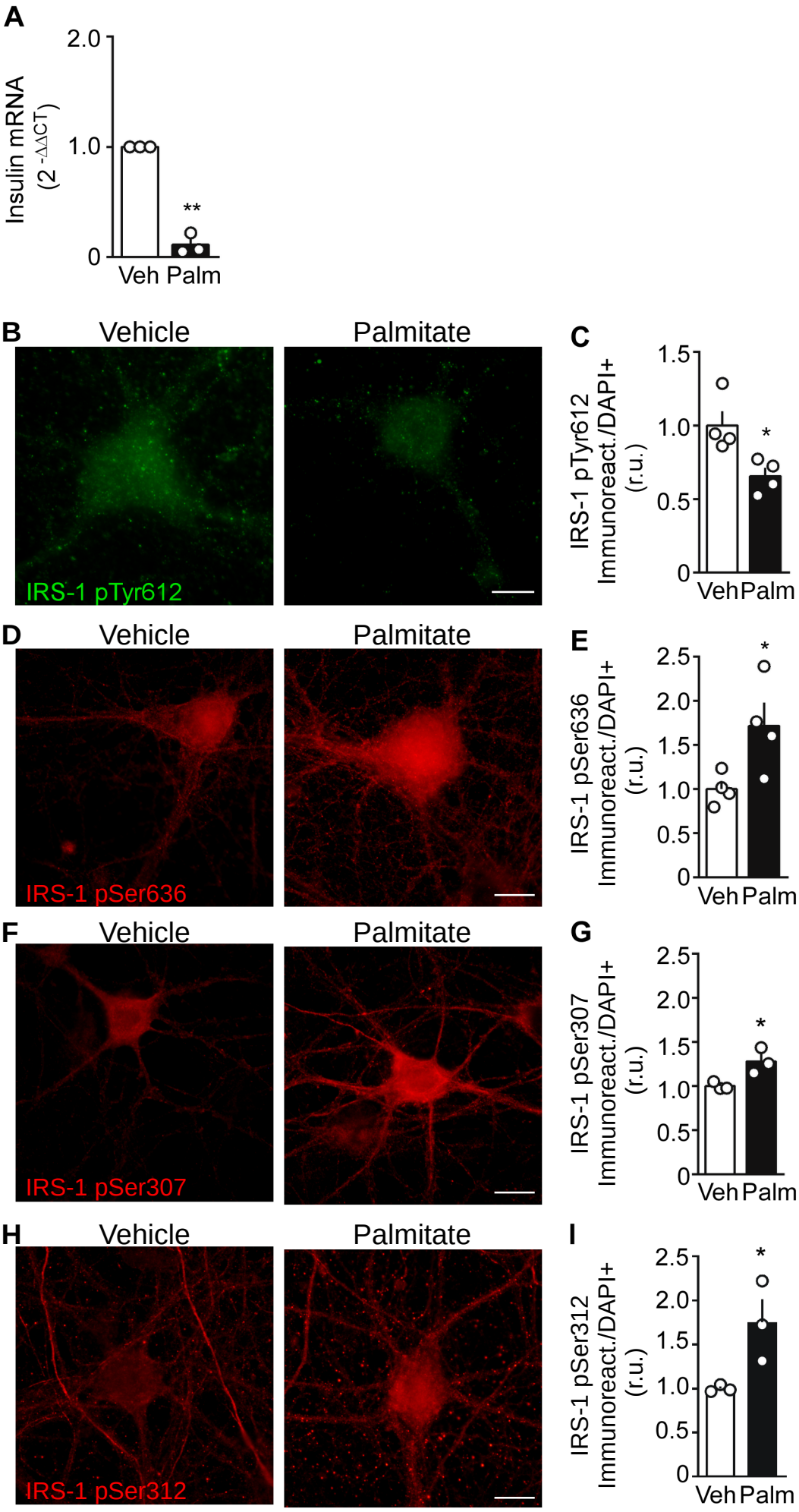
A
Insulin mRNA
(2 -ΔΔCT)
2.0
1.0
0
**
Veh Palm
B
Vehicle
Palmitate
IRS-1 pTyr612
C
IRS-1 pTyr612
Immunoreact./DAPI+
(r.u.)
1.5
1.0
0.5
0
*
Veh Palm
D
Vehicle
Palmitate
IRS-1 pSer636
E
IRS-1 pSer636
Immunoreact./DAPI+
(r.u.)
2.5
2.0
1.5
1.0
0.5
0
*
Veh Palm
F
Vehicle
Palmitate
IRS-1 pSer307
G
IRS-1 pSer307
Immunoreact./DAPI+
(r.u.)
2.5
2.0
1.5
1.0
0.5
0
*
Veh Palm
H
Vehicle
Palmitate
IRS-1 pSer312
I
IRS-1 pSer312
Immunoreact./DAPI+
(r.u.)
2.5
2.0
1.5
1.0
0.5
0
*
Veh Palm

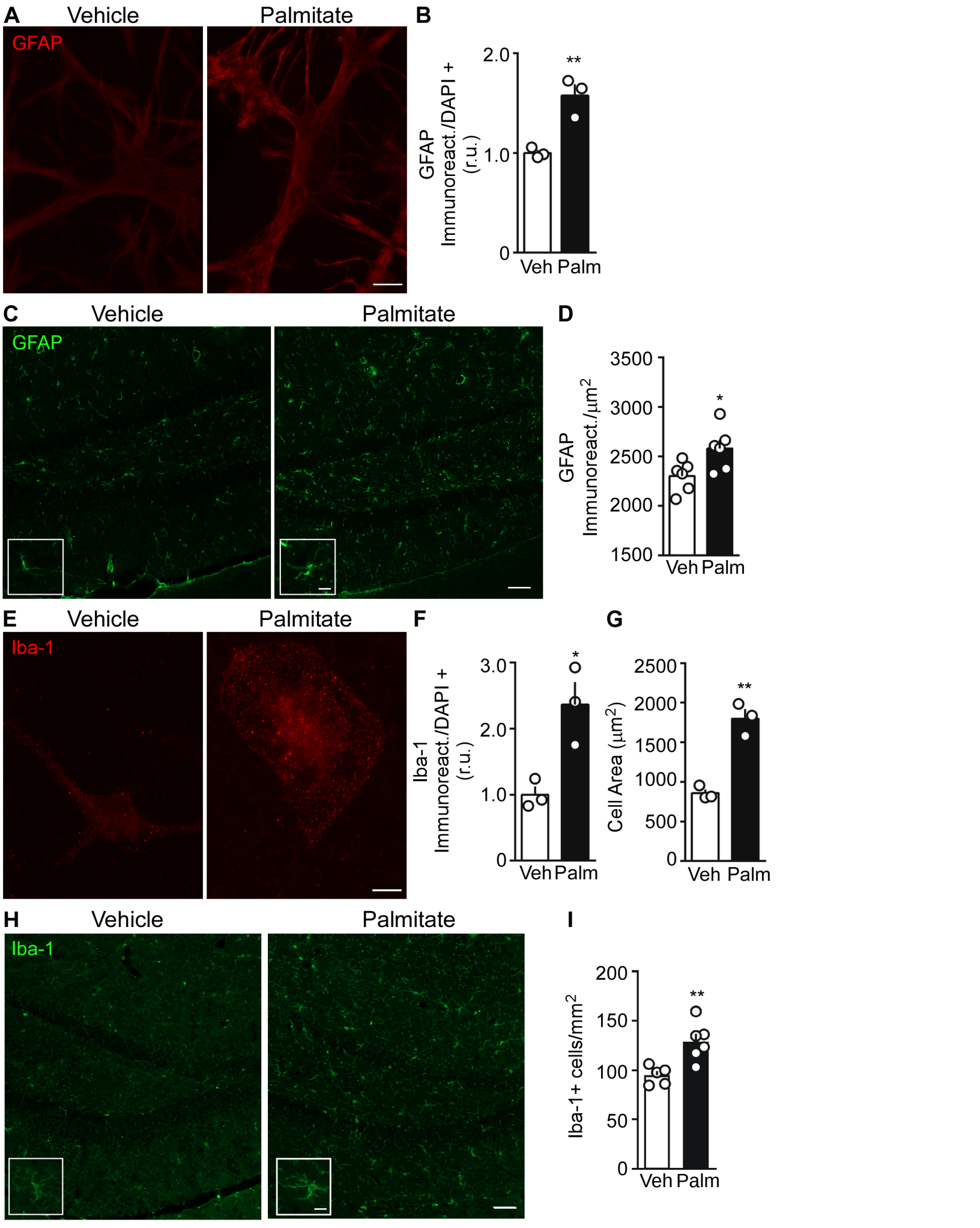


Melo et al., 2019 - Figure 4

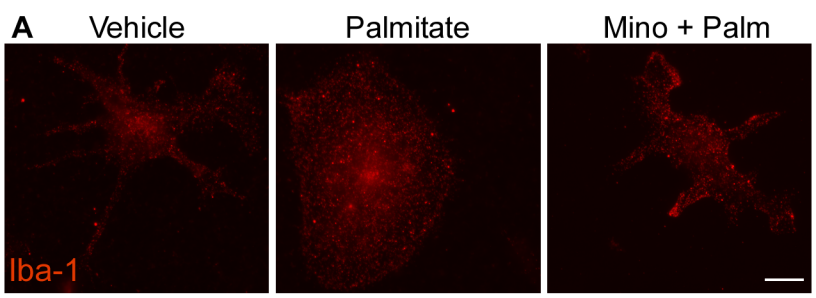


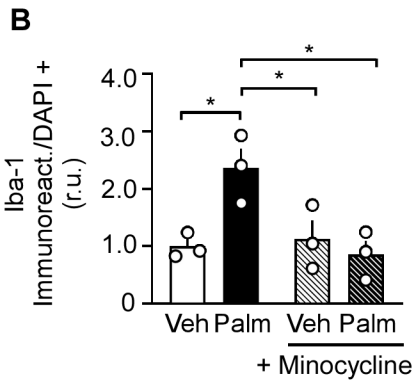


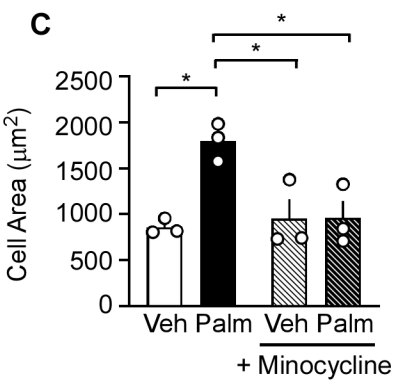


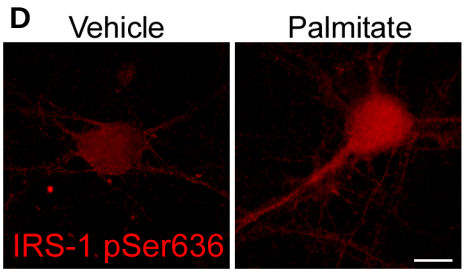


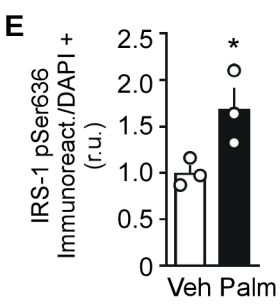


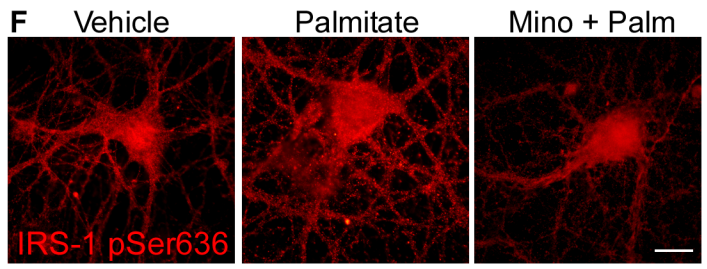


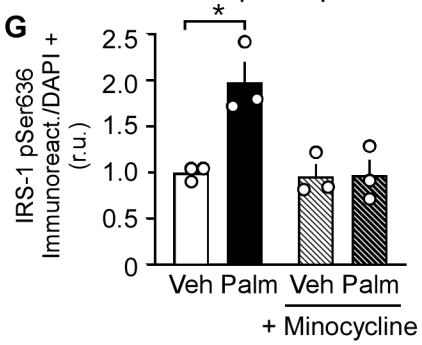


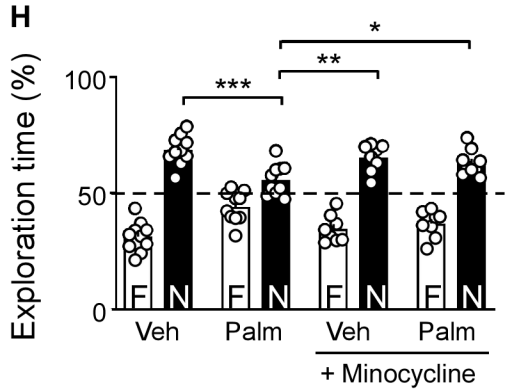


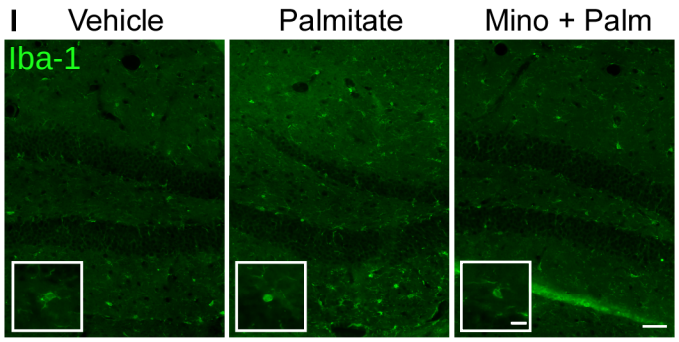


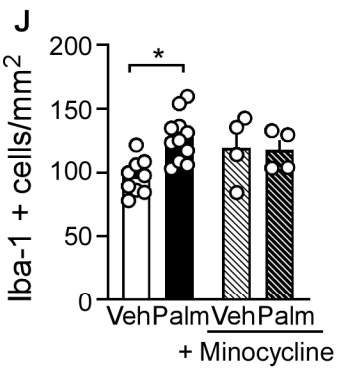


Melo et al., 2019 - Figure 5

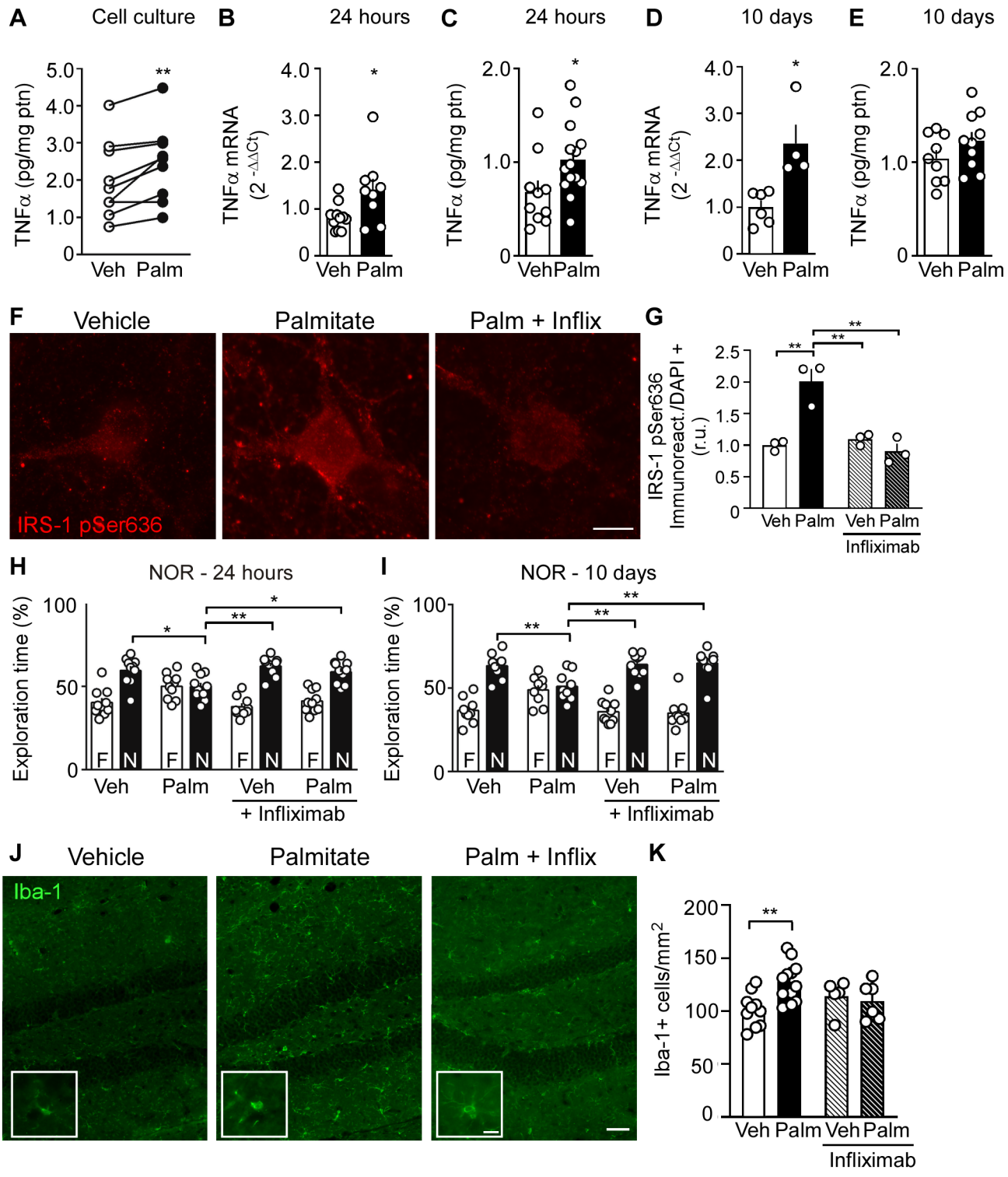
A
Cell culture
TNFα (pg/mg ptn)
Veh Palm
B
24 hours
TNFα mRNA (2 -ΔΔCt)
Veh Palm
C
24 hours
TNFα (pg/mg ptn)
Veh Palm
D
10 days
TNFα mRNA (2 -ΔΔCt)
Veh Palm
E
10 days
TNFα (pg/mg ptn)
Veh Palm
F
Vehicle
Palmitate
Palm + Inflix
IRS-1 pSer636
G
IRS-1 pSer636 Immunoreact./DAPI + (r.u.)
Veh Palm Veh Palm
Infliximab
H
NOR - 24 hours
Exploration time (%)
F N F N F N F N
Veh Palm Veh Palm
+ Infliximab
I
NOR - 10 days
Exploration time (%)
F N F N F N F N
Veh Palm Veh Palm
+ Infliximab
J
Vehicle
Palmitate
Palm + Inflix
Iba-1
K
Iba-1+ cells/mm2
Veh Palm Veh Palm
Infliximab

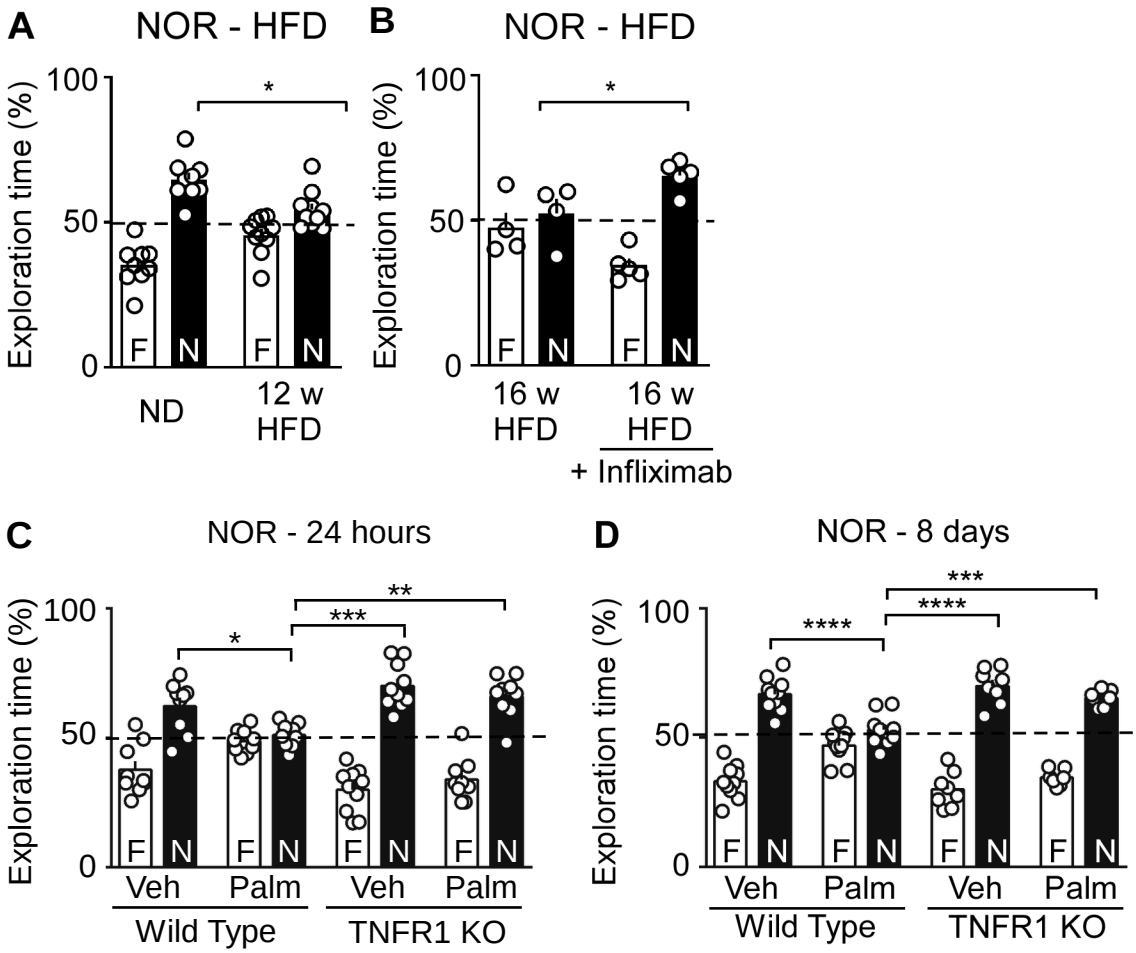
A
NOR - HFD
B
NOR - HFD
Exploration time (%)
100
50
0
*
F
N
ND
12 w HFD
16 w HFD
16 w HFD + Infliximab
C
NOR - 24 hours
D
NOR - 8 days
**
***
****
Veh
Palm
Wild Type
TNFR1 KO

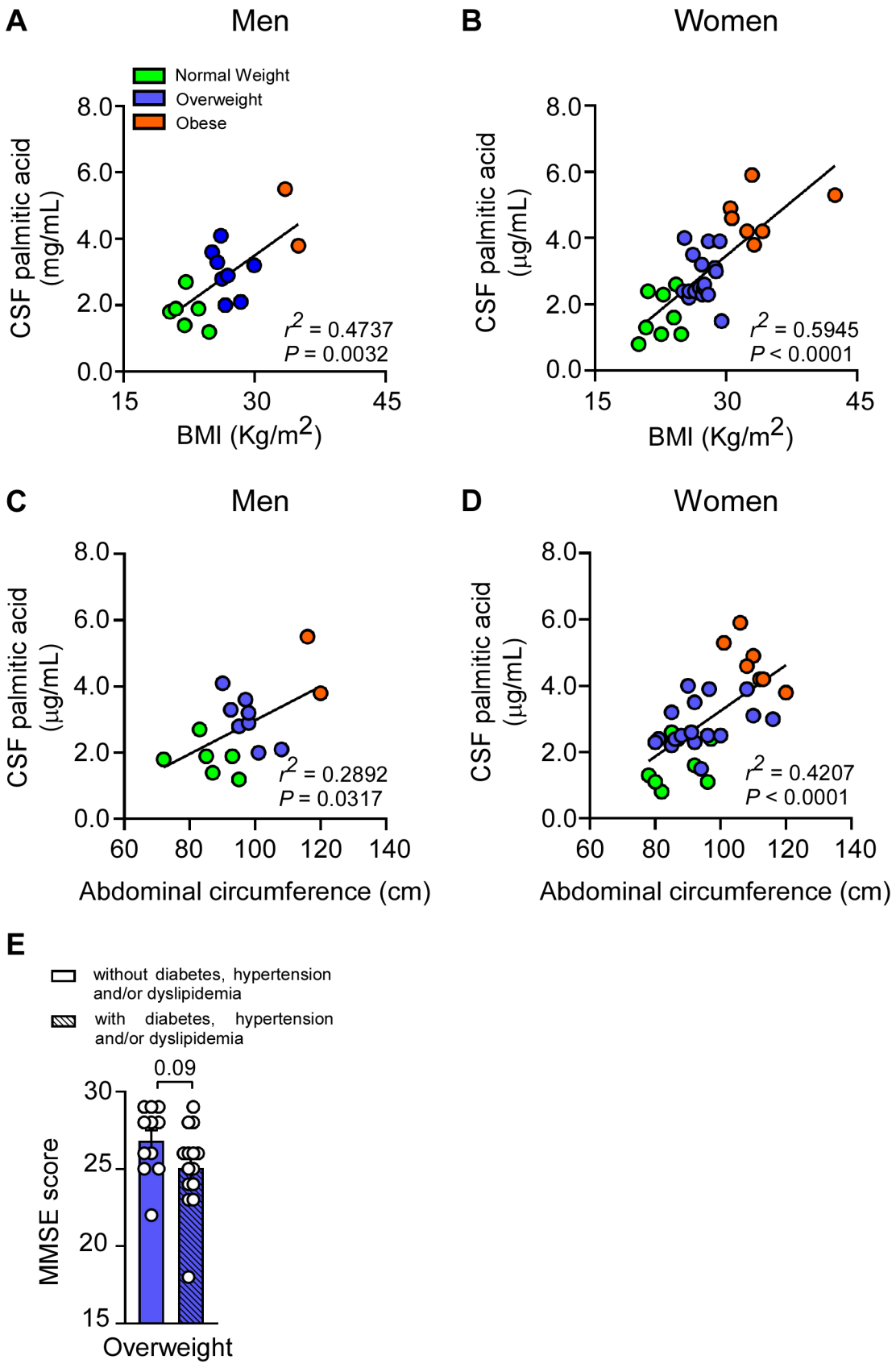
A
Men
Normal Weight
Overweight
Obese
CSF palmitic acid (mg/mL)
8.0
6.0
4.0
2.0
0.0
15
30
45
BMI (Kg/m2)
r2 = 0.4737
P = 0.0032
B
Women
CSF palmitic acid (μg/mL)
r2 = 0.5945
P < 0.0001
C
Men
CSF palmitic acid (μg/mL)
60
80
100
120
140
Abdominal circumference (cm)
r2 = 0.2892
P = 0.0317
D
Women
r2 = 0.4207
P < 0.0001
E
without diabetes, hypertension and/or dyslipidemia
with diabetes, hypertension and/or dyslipidemia
0.09
MMSE score
30
25
20
15
Overweight

**Figure S1. Related to Figure 1. CSF palmitic acid correlates with BMI and abdominal circumference in females and males.**

**(A, B)** Correlation between CSF palmitic acid and BMI in men (N= 16) (**A**) and women (N = 33) (**B**); linear regression, $r^2$ and p values as indicated.

**(C, D)** Correlation between CSF palmitic acid and abdominal circumference in men (N = 16) (**A**) and women (N = 33) (**B**); linear regression, $r^2$ and p values as indicated.

**(E)** MMSE scores in overweigh subjects according to absence (N = 11) or presence (N = 14) of diabetes, hypertension or dyslipidemia. p = 0.09 (unpaired t-test).

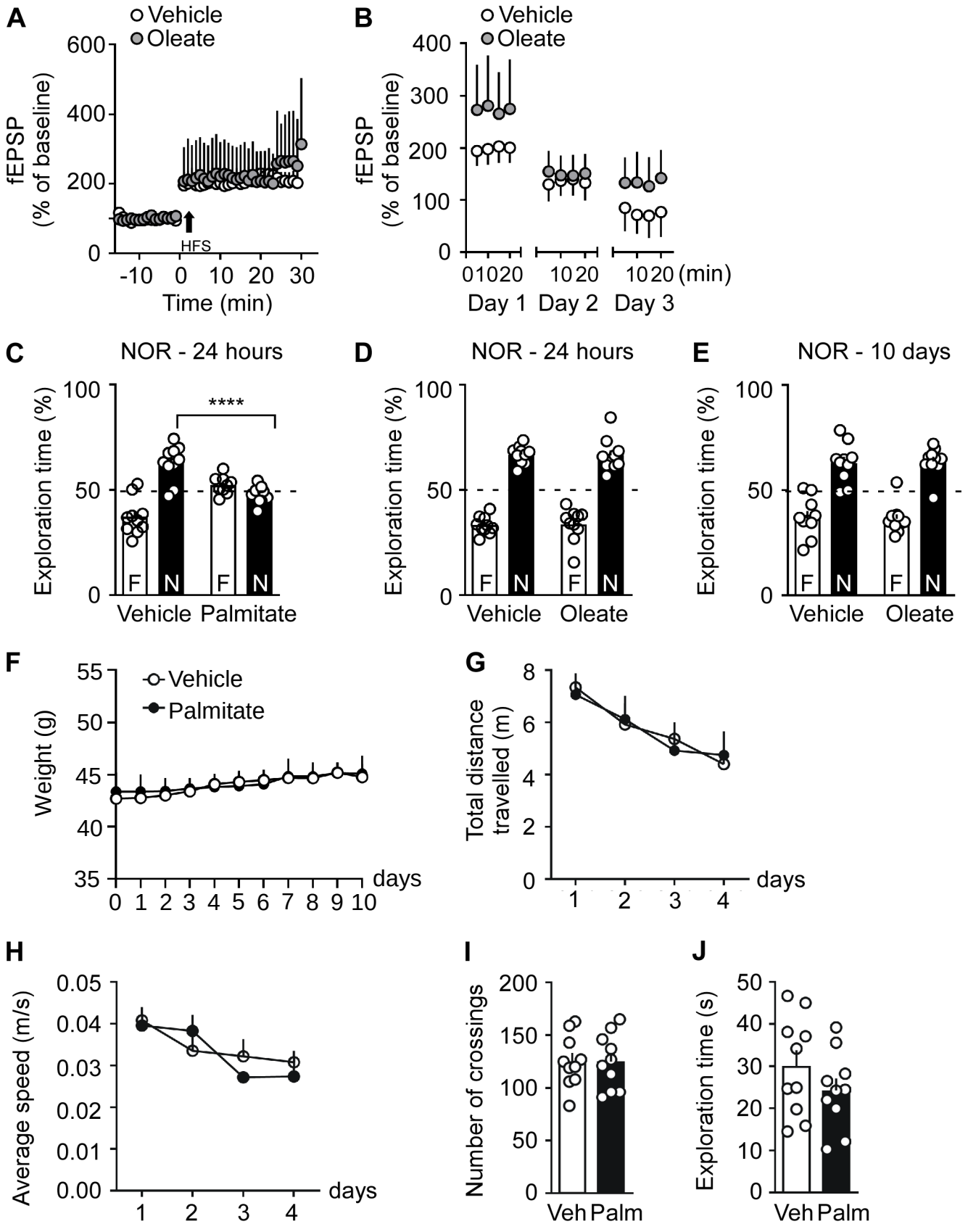
A
Vehicle
Oleate
fEPSP (% of baseline)
600
400
200
0
HFS
-10 0 10 20 30
Time (min)
B
Vehicle
Oleate
fEPSP (% of baseline)
400
300
200
100
0
0 10 20 0 10 20 0 10 20 (min)
Day 1 Day 2 Day 3
C
NOR - 24 hours
Exploration time (%)
100
50
0
****
F N F N
Vehicle Palmitate
D
NOR - 24 hours
Exploration time (%)
100
50
0
F N F N
Vehicle Oleate
E
NOR - 10 days
Exploration time (%)
100
50
0
F N F N
Vehicle Oleate
F
Vehicle
Palmitate
Weight (g)
55
50
45
40
35
0 1 2 3 4 5 6 7 8 9 10
days
G
Total distance travelled (m)
8
6
4
2
0
1 2 3 4
days
H
Average speed (m/s)
0.05
0.04
0.03
0.02
0.01
0.00
1 2 3 4
days
I
Number of crossings
200
150
100
50
0
Veh Palm
J
Exploration time (s)
50
40
30
20
10
0
Veh Palm

**Figure S2. Related to Figure 2. Oleate does not inhibit long-term potentiation and does not impair memory in mice.**

(**A, B**) Long-term potentiation (LTP) was induced by high-frequency stimulation (HFS, arrow) at the CA3 hippocampal subregion and recording in CA1 in awake freely-moving male 3-5-month-old mice, 10 days after intrahippocampal infusion of vehicle or oleate (0.3 nmol). (**A**) Measurements performed immediately following HFS. (**B**) Measurements performed on subsequent days following LTP induction. N = 6 vehicle-infused/N= 4 oleate-infused mice. Vehicle condition was showed in Figure 2 A,C.

(**C**) Novel object recognition (NOR) test in male 3-5-month-old mice infused i.c.v. with vehicle or palmitate (3 nmol). Testing was performed 24 hours after infusion. Bars (means ± SEM) represent time spent exploring the familiar (F) or novel (N) objects and symbols represent individual animals. ***$p < 0.001$ (unpaired t-test).

(**D,E**) Novel object recognition (NOR) test in male 3 month-old mice infused i.c.v. with vehicle or oleate (3 nmol). Testing was performed 24 hours (A) or 10 days (B) after infusion. Bars (means ± SE) represent time spent exploring the familiar (F) or novel (N) objects and symbols represent individual animals.

**(F)** Average body weights over ten days following i.c.v. infusion of vehicle or palmitate in mice (N= 6- vehicle-infused mice, N = 5 palmitate-infused mice).

**(G)** Total distance travelled (m) in the training phase of the Barnes maze for vehicle- or palmitate infused 3-5-month-old male mice. Symbols represent means ± standard errors. N = 7 vehicle-infused/6 palmitate-infused mice.

**(H**) Average speed (m/s) in the training phase of the Barnes maze for vehicle- or palmitate infused 3-5-month-old male mice. Symbols represent means ± standard errors. N = 7 vehicle-infused/6 palmitate-infused mice.

**(I)** Number of crossings in the open field test for male 3-5-month-old mice infused i.c.v. with vehicle or palmitate (3 nmol). Testing was performed 10 days after infusion. Bars represent means ± SEM and symbols represent individual animals.

**(J)** Total exploration time in the novel object recognition (NOR) test for male 3-5-month-old mice infused i.c.v. with vehicle or palmitate (3 nmol). Testing was performed 10 days after infusion. Bars represent means ± SEM and symbols represent individual animals.

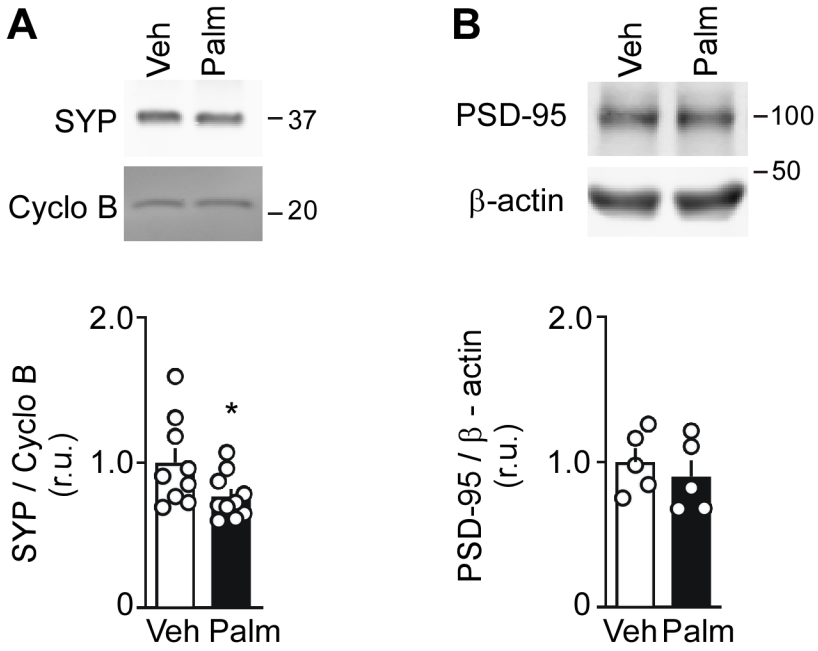
A
Veh
Palm
SYP
37
Cyclo B
20
SYP / Cyclo B
(r.u.)
2.0
1.0
0
*
Veh Palm
B
Veh
Palm
PSD-95
100
50
β-actin
PSD-95 / β - actin
(r.u.)
2.0
1.0
0
Veh Palm

**Figure S3. Related to Figure 2. Palmitate induces a reduction in synaptophysin but not PSD-95 immunoreactivities (10 days post-infusion) in the mouse hippocampus.**

**(A)** Immunoblot analysis of synaptophysin (SYP; normalized by cyclophilin B) in hippocampal homogenates of 3-5-month-old mice infused i.c.v. with vehicle or palmitate (3 nmol) 10 days before collection of hippocampi. Bars represent means ± standard errors and symbols represent individual animals. *$p < 0.05$ (unpaired t-test).

**(B)** Immunoblot analysis of PSD-95 (normalized by β-actin) in hippocampal homogenates of 3-5-month-old mice infused i.c.v. with vehicle or palmitate (3 nmol) 10 days before collection of hipocampi. Bars represent means ± SE and symbols represent individual animals.

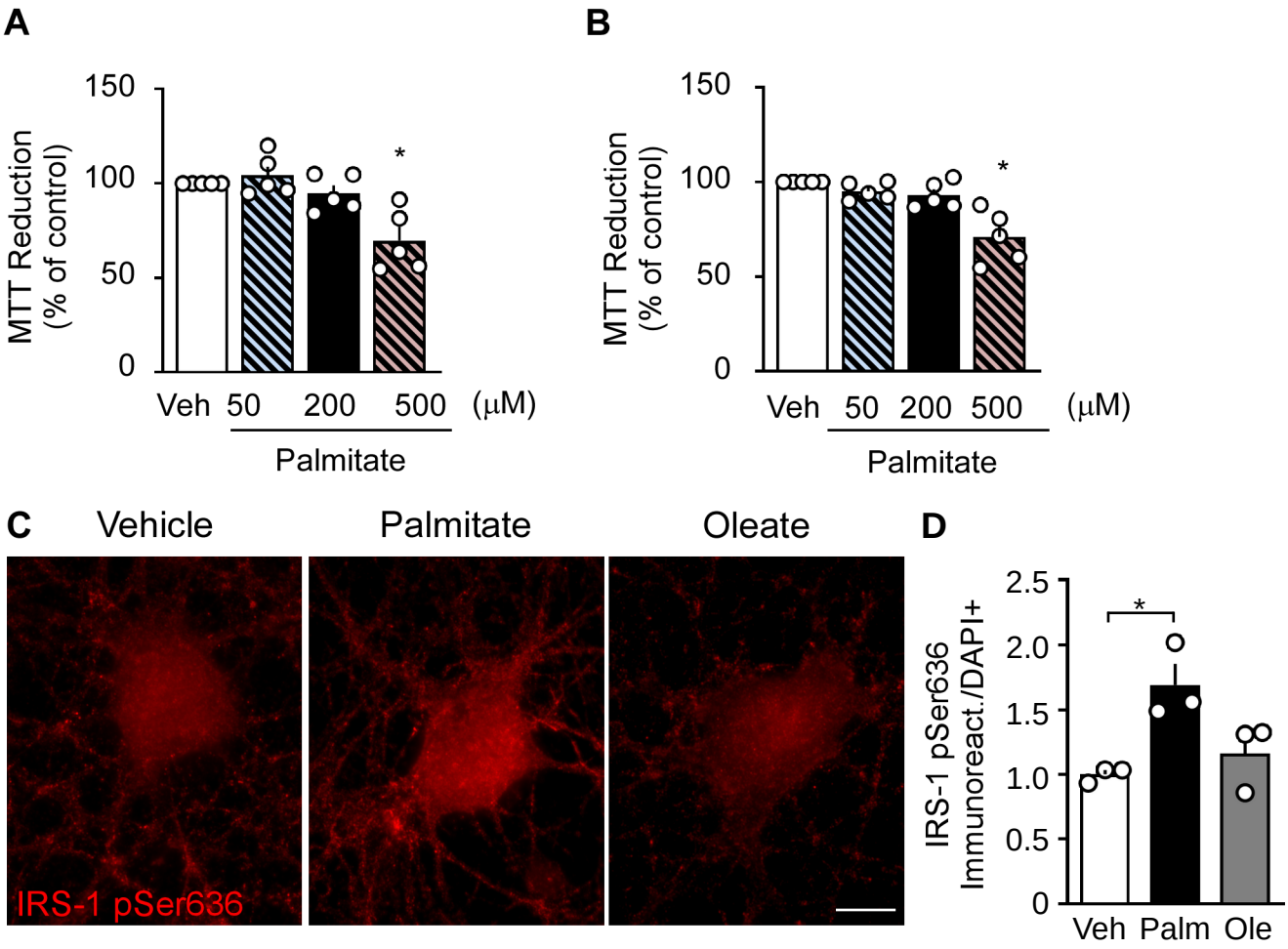
A
B
MTT Reduction
(% of control)
150
100
50
0
Veh
50
200
500
(μM)
Palmitate
*
C
Vehicle
Palmitate
Oleate
IRS-1 pSer636
D
IRS-1 pSer636
Immunoreact./DAPI+
2.5
2.0
1.5
1.0
0.5
0
Veh
Palm
Ole

**Figure S4. Related to Figure 3. Palmitate (up to 200 μM) does not affect cell viability, and oleate does not increase IRS-1pSer636 phosphorylation in hippocampal cultures.**

**(A,B)** MTT reduction in hippocampal cultures exposed to vehicle or increasing concentrations of palmitate (50 to 500 μM) for 24 hours (**A**) or 48 hours (**B**). Bars represent means ± SEM and symbols represent experiments with 5 independent cultures. *$p < 0.05$ (one-way ANOVA followed by Dunnett's post hoc test compared to control).

**(C-D)** Neuronal IRS-1pSer636 immunolabeling in cultured hippocampal neurons exposed to vehicle, palmitate (200 μM) or oleate (200 μM) for 4 hours (10-30 images analyzed per experimental condition per experiment using independent neuronal cultures). Scale bar = 10 μm. Bars represent means ± standard errors and symbols represent independent cultures. *$p < 0.05$ (one-way ANOVA followed by Holm-Sidak's post hoc test).

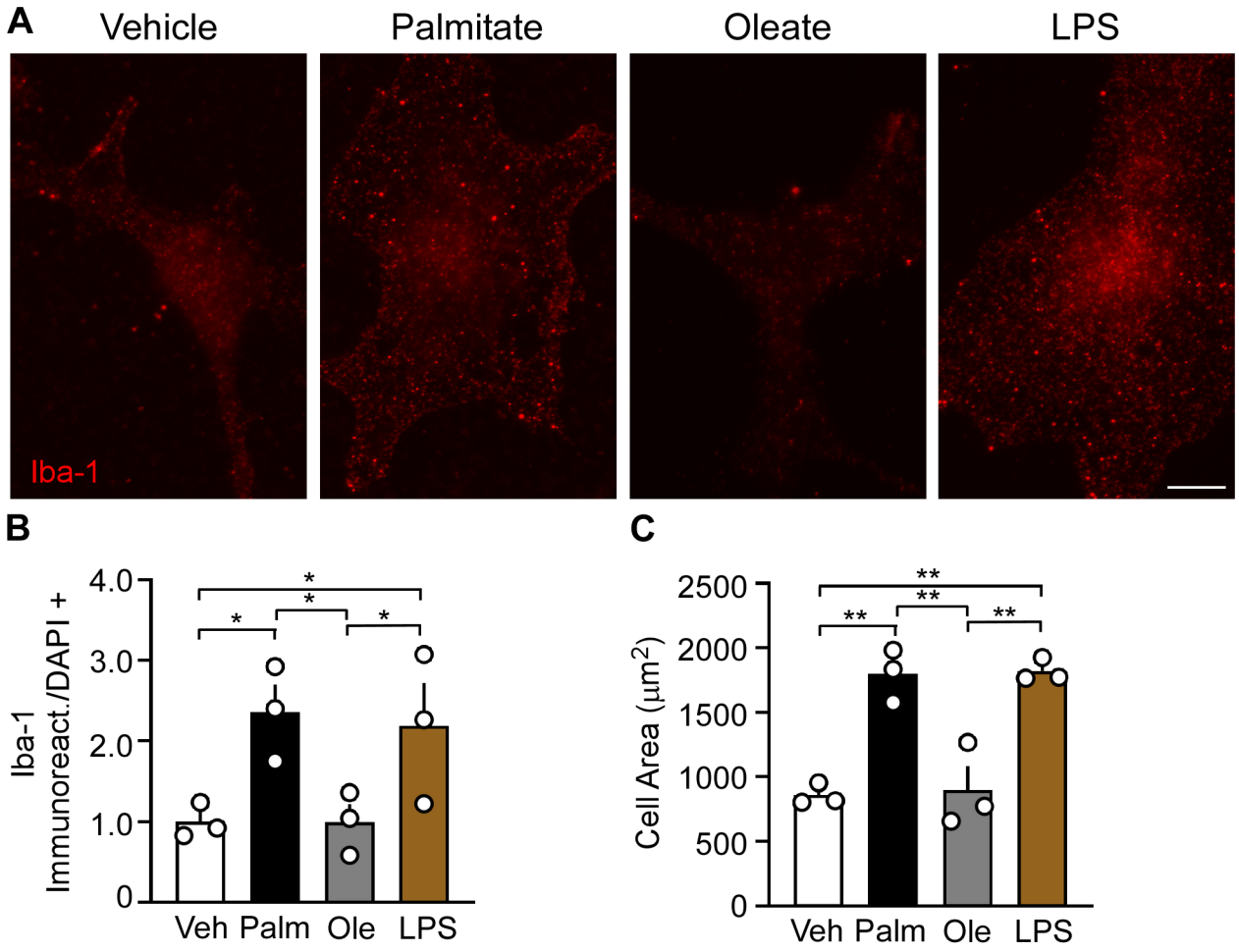
A
Vehicle
Palmitate
Oleate
LPS
Iba-1
B
Iba-1 Immunoreact./DAPI +
4.0
3.0
2.0
1.0
0
*
*
*
*
Veh
Palm
Ole
LPS
C
Cell Area (µm2)
2500
2000
1500
1000
500
0
**
**
**
**
Veh
Palm
Ole
LPS

**Figure S5. Related to Figure 4. Oleate has no effect on Iba-1 immunoreactivity or average cell area in microglial cultures.**

**(A)** Representative images of Iba-1 immunolabeling in purified microglial cultures exposed to vehicle, 200 μM palmitate, 200 μM oleate or LPS (100 ng/ml, used as a positive control for microglial activation) for 2 hours. Scale bar = 10 μm.

**(B,C)** Iba-1 immunoreactivity (B) and cell area (C) in purified microglial cultures exposed to vehicle, 200 μM palmitate, 200 μM oleate or LPS (100 ng/ml, used as a positive control for microglial activation) for 2 hours. Bars represent means ± standard errors and symbols represent independent cultures. *$p < 0.05$; **$p < 0.005$ (one-way ANOVA followed by Holm-Sidak's post hoc test). Vehicle and palmitate conditions were showed in Figure 4 F,G.

**Table S1. Related to Figure 1.** Patient demographics for C16:0 and obesity studies.

| Case # | Age | Gender | Education | DM | DLP | H | Weight (Kg) | Height (m) | BMI | Abdominal Circumference | C16:0 (ug/mL) | MMSE score |
|---|---|---|---|---|---|---|---|---|---|---|---|---|
| 50 | 46 | F | 9 | 0 | 0 | 0 | 57.7 | 1.70 | 20.0 | 82.0 | 0.8 | 17 |
| 127 | 73 | M | 12 | 0 | 0 | 1 | 55.3 | 1.65 | 20.3 | 72.0 | 1.8 | 30 |
| 99 | 73 | F | 8 | 0 | 0 | 0 | 50.0 | 1.55 | 20.8 | 78.0 | 1.3 | 21 |
| 148 | 71 | M | 2 | 0 | 0 | 0 | 59.9 | 1.69 | 21.0 | 85.0 | 1.9 | 25 |
| 138 | 71 | F | 7 | 0 | 0 | 0 | 54.5 | 1.61 | 21.0 | 97.0 | 2.4 | 25 |
| 1 | 66 | M | 8 | 0 | 0 | 0 | 61.3 | 1.67 | 22.0 | 87.0 | 1.4 | 30 |
| 236 | 67 | M | 3 | 0 | 0 | 0 | 61.0 | 1.66 | 22.1 | 83.0 | 2.7 | 27 |
| 227 | 64 | F | 8 | 0 | 0 | 0 | 53.5 | 1.54 | 22.6 | 80.0 | 1.1 | 25 |
| 78 | 65 | F | 2 | 0 | 0 | 0 | 57.6 | 1.59 | 22.8 | 85.5 | 2.3 | 24 |
| 114 | 77 | M | 11 | 0 | 0 | 0 | 72.2 | 1.75 | 23.6 | 93.0 | 1.9 | 29 |
| 195 | 73 | F | 11 | 1 | 1 | 1 | 54.0 | 1.50 | 24.0 | 92.0 | 1.6 | 27 |
| 225 | 73 | F | 4 | 0 | 0 | 0 | 58.3 | 1.55 | 24.2 | 85.0 | 2.6 | 25 |
| 22 | 65 | M | 4 | 0 | 0 | 0 | 72.5 | 1.71 | 24.8 | 95.0 | 1.2 | 20 |
| 7 | 59 | F | 11 | 0 | 0 | 0 | 60.5 | 1.56 | 24.8 | 96.0 | 1.1 | 26 |
| 88 | 65 | F | 9 | 1 | 0 | 1 | 57.2 | 1.51 | 25.1 | 81.0 | 2.4 | 29 |
| 84 | 80 | M | 0 | 0 | 1 | 1 | 81.4 | 1.80 | 25.1 | 97.0 | 3.6 | 28 |
| 139 | 72 | F | 4 | 0 | 1 | 0 | 67.0 | 1.63 | 25.2 | 90.0 | 4.0 | 23 |
| 27 | 71 | M | 0 | 0 | 0 | 1 | 70.0 | 1.65 | 25.7 | 92.5 | 3.3 | 24 |
| 3 | 79 | F | 15 | 0 | 0 | 0 | 57.1 | 1.49 | 25.7 | 85.0 | 2.2 | 29 |
| 203 | 74 | F | 3 | 0 | 0 | 0 | 65.9 | 1.60 | 25.7 | 87.0 | 2.4 | 28 |
| 45 | 66 | M | 27 | 0 | 1 | 1 | 80.0 | 1.75 | 26.1 | 90.0 | 4.1 | 26 |
| 4 | 57 | F | 11 | 0 | 0 | 0 | 71.3 | 1.65 | 26.2 | 92.0 | 3.5 | 29 |
| 66 | 64 | M | 4 | 1 | 1 | 1 | 69.8 | 1.63 | 26.3 | 95.0 | 2.8 | 25 |
| 130 | 69 | F | 14 | 0 | 1 | 1 | 58.6 | 1.49 | 26.4 | 86.0 | 2.4 | 26 |
| 96 | 73 | M | 15 | 0 | 0 | 0 | 80.6 | 1.74 | 26.6 | 101.0 | 2.0 | 25 |
| 77 | 67 | M | 12 | 0 | 0 | 1 | 77.8 | 1.70 | 26.9 | 98.0 | 2.9 | 26 |

| | | | | | | | | | | | | |
|---|---|---|---|---|---|---|---|---|---|---|---|---|
| 137 | 62 | F | 6 | 0 | 0 | 0 | 64.8 | 1.55 | 27.0 | 88.0 | 2.5 | 26 |
| 226 | 64 | F | 4 | 1 | 0 | 1 | 62.8 | 1.52 | 27.2 | 85.0 | 3.2 | 25 |
| 103 | 69 | F | 5 | 0 | 0 | 1 | 66.4 | 1.56 | 27.3 | 92.0 | 2.3 | 26 |
| 98 | 68 | F | 4 | 0 | 0 | 0 | 65.9 | 1.55 | 27.4 | 96.0 | 2.5 | 26 |
| 230 | 65 | F | 8 | 0 | 0 | 0 | 72.0 | 1.62 | 27.4 | 100.0 | 2.5 | 28 |
| 105 | 63 | F | 9 | 0 | 0 | 1 | 69.5 | 1.59 | 27.5 | 91.0 | 2.6 | - |
| 228 | 65 | F | 5 | 0 | 0 | 0 | 56.3 | 1.42 | 27.9 | 80.0 | 2.3 | 22 |
| 224 | 74 | F | 4 | 0 | 0 | 1 | 63.8 | 1.51 | 28.0 | 96.5 | 3.9 | 18 |
| 65 | 78 | M | 6 | 1 | 1 | 1 | 75.5 | 1.63 | 28.4 | 108.0 | 2.1 | 28 |
| 92 | 64 | F | 13 | 0 | 1 | 1 | 81.0 | 1.68 | 28.7 | 110.0 | 3.1 | 24 |
| 167 | 73 | F | 4 | 0 | 0 | 1 | 78.5 | 1.65 | 28.8 | 116.0 | 3.0 | 23 |
| 194 | 68 | F | 23 | 0 | 0 | 0 | 79.7 | 1.65 | 29.3 | 108.0 | 3.9 | 25 |
| 231 | 59 | F | 8 | 0 | 0 | 0 | 65.4 | 1.49 | 29.5 | 94.0 | 1.5 | 28 |
| 101 | 66 | M | 17 | 0 | 0 | 0 | 71.1 | 1.54 | 30.0 | 98.0 | 3.2 | 29 |
| 150 | 75 | F | 5 | 0 | 0 | 1 | 78.0 | 1.60 | 30.5 | 110.0 | 4.9 | 27 |
| 81 | 71 | F | 5 | 0 | 0 | 0 | 80.5 | 1.62 | 30.7 | 108.0 | 4.6 | 27 |
| 76 | 63 | F | 4 | 1 | 1 | 1 | 70.0 | 1.47 | 32.4 | 112.0 | 4.2 | 22 |
| 145 | 59 | F | 14 | 0 | 0 | 0 | 84.4 | 1.60 | 33.0 | 106.0 | 5.9 | 28 |
| 170 | 65 | F | 5 | 0 | 0 | 0 | 85.0 | 1.60 | 33.2 | 120.0 | 3.8 | 24 |
| 153 | 77 | M | 12 | 1 | 0 | 1 | 89.0 | 1.63 | 33.5 | 116.0 | 5.5 | 26 |
| 240 | 76 | F | 4 | 1 | 1 | 0 | 82.1 | 1.55 | 34.2 | 113.0 | 4.2 | 28 |
| 100 | 65 | M | 8 | 1 | 1 | 0 | 104.8 | 1.73 | 35.0 | 120.0 | 3.8 | 28 |
| 95 | 66 | F | 8 | 1 | 1 | 1 | 98.2 | 1.52 | 42.5 | 101.0 | 5.3 | - |

The numbers 0 or 1 indicates absence (0) or presence (1) of diabetes mellitus (DM), dyslipidemia (DLP) or hypertension (H);
BMI: Body mass index;
MMSE: Mini-Mental State Exam

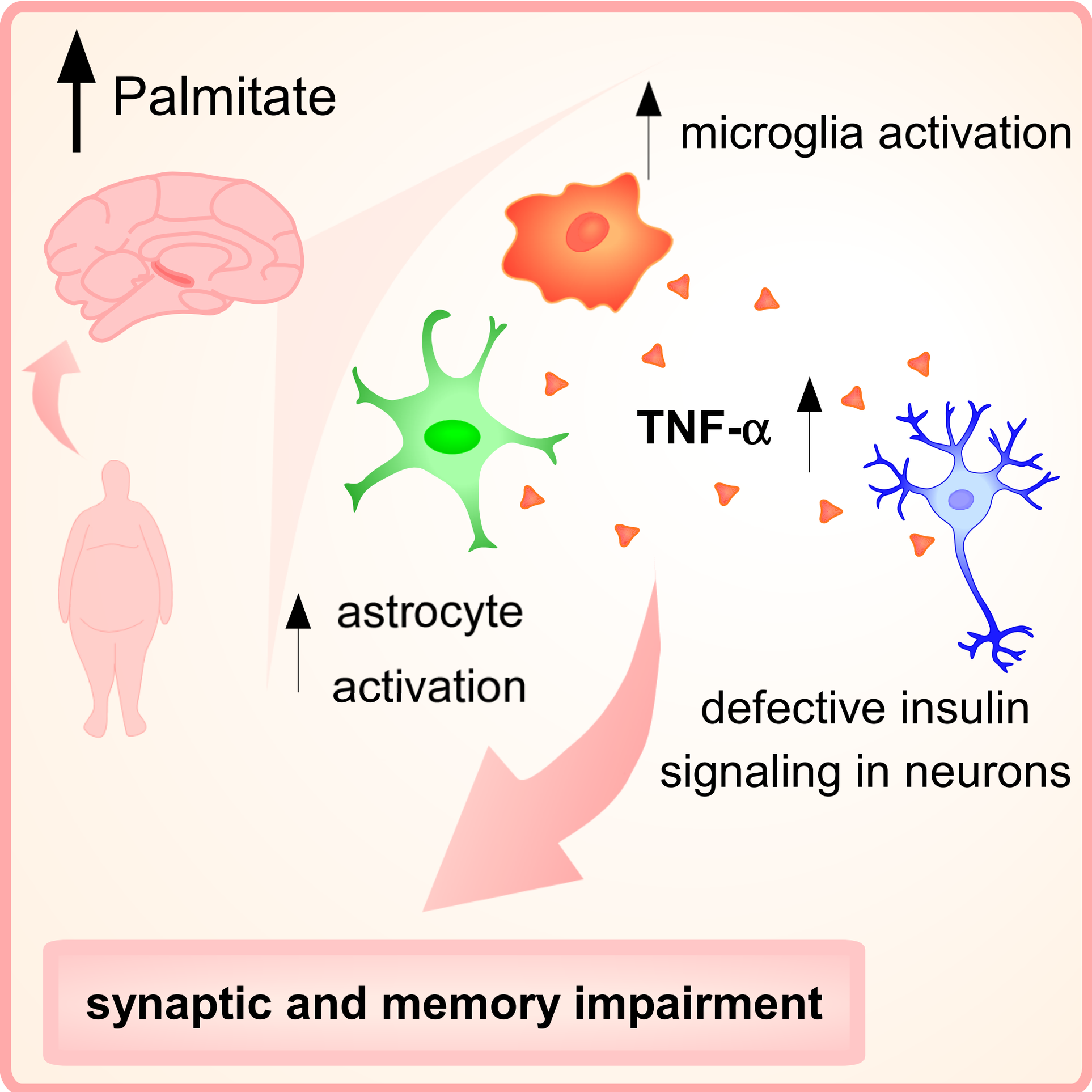
Palmitate
microglia activation
TNF-α
astrocyte
activation
defective insulin
signaling in neurons
synaptic and memory impairment